

Identification and Spatiotemporal Control of the Asymmetrical Membrane Cortex in Cleavage Stage Sea Urchin Embryos

Author: Lea Marie Alford

Persistent link: <http://hdl.handle.net/2345/978>

This work is posted on [eScholarship@BC](#),
Boston College University Libraries.

Boston College Electronic Thesis or Dissertation, 2009

Copyright is held by the author, with all rights reserved, unless otherwise noted.

Boston College
The Graduate School of Arts and Sciences
Department of Biology

**IDENTIFICATION AND SPATIOTEMPORAL CONTROL
OF THE ASYMMETRICAL MEMBRANE CORTEX
IN CLEAVAGE STAGE SEA URCHIN EMBRYOS**

a dissertation

by

LEA MARIE ALFORD

submitted in partial fulfillment of the requirements

for the degree of

Doctor of Philosophy

December 2009

© copyright by LEA MARIE ALFORD
2009

Abstract

IDENTIFICATION AND SPATIOTEMPORAL CONTROL OF THE ASYMMETRICAL MEMBRANE CORTEX IN CLEAVAGE STAGE SEA URCHIN EMBRYOS

By Lea Marie Alford

Advisor: David R. Burgess

Polarity established by the first cleavages in sea urchin embryos was investigated in this thesis revealing precocious embryonic polarity. Studies of embryonic polarity have focused on protostomes such as *C. elegans*, and those on deuterostomes have focused on later developmental stages. I find asymmetries in the sea urchin membrane cell cortex as early as the first division after fertilization as a result of new membrane addition in the cleavage furrow. Membrane domains and the polarity determinants Par6, aPKC, and Cdc42 are polarized to the apical, or free, cell surface, while the cell-cell contact site remains distinct. Using immunofluorescence, fluorescence recovery after photobleaching (FRAP), and specific inhibitor treatments, myosin filaments were identified as the major regulator of membrane cortex polarity. However, membrane domains and cortical polarity determinants are differentially regulated with respect to blastomere dissociation. These asymmetries are required for proper spindle alignment and cleavage plane determination and are responsible for polarized fluid phase endocytosis. The work in this thesis and future studies addressing the connection between the membrane cortex and myosin filaments has and will lead to a greater

understanding of the maintenance of embryonic polarity in cleavage stage sea urchin embryos.

TABLE OF CONTENTS

CHAPTER 1: INTRODUCTION	1
INTRODUCTION.....	1
BACKGROUND.....	3
<i>EMBRYONIC, PLANAR CELL, AND CELL POLARITY</i>	3
<i>POLARITY DURING ECHINODERMN DEVELOPMENT</i>	7
SPECIFIC AIMS.....	9
CHAPTER 2: CELL POLARITY EMERGES AT FIRST CLEAVAGE IN SEA URCHIN EMBRYOS.....	10
INTRODUCTION.....	10
RESULTS.....	13
<i>CELL SURFACE AND CORTICAL MARKERS ARE POLARIZED BY CYTOKINESIS AND RETAINED ON THE FORMER EGG MEMBRANE</i>	13
<i>POLARIZED PLASMA MEMBRANE DOMAINS ARE INDEPENDENT OF Ca^{2+}-DEPENDENT CELL ADHESION AND ACTIN BUT DEPENDENT ON MYOSIN FILAMENT ASSEMBLY</i>	15
<i>MEMBRANE LIPIDS ARE SEGREGATED BY CLEAVAGE AND REMAIN DISTINCT AFTER MEMBRANE MANIPULATION</i>	17
<i>Ca^{2+}-MEDIATED CELL ADHESION, THE ACTIN CYTOSKELETON, AND FUNCTIONAL APKC ARE REQUIRED FOR PAR6 LOCALIZATION</i>	18
<i>FUNCTIONAL POLARITY EXISTS AT THE EARLY CLEAVAGE STAGES</i>	20
DISCUSSION	22
FIGURES	26
CHAPTER 3: SPATIOTEMPORAL CONTROL OF THE ASYMMETRICAL MEMBRANE CORTEX IN CLEAVAGE STAGE SEA URCHIN EMBRYOS	40
INTRODUCTION.....	40
RESULTS.....	46
<i>GANGLIOSIDE G_{M1} BECOMES MOBILE IN THE MEMBRANE CORTEX AT MID-ANAPHASE</i>	46
<i>MYOSIN FILAMENTS PROVIDE SCAFFOLDING FOR G_{M1} IN THE MEMBRANE CORTEX</i>	48
<i>MYOSIN DISTRIBUTION CHANGES IN DISSOCIATED BLASTOMERES</i>	51
<i>MYOSIN LIGHT CHAIN KINASE PROVIDES SCAFFOLDING FOR POLARITY PROTEINS PAR6, APKC, AND CDC42</i>	53
DISCUSSION	54
FIGURES	58
CHAPTER 4: DISCUSSION.....	76
CHAPTER 5: MATERIALS AND METHODS.....	83
CHAPTER 6: REFERENCES	90

LIST OF FIGURES AND TABLES

FIGURE 1: GANGLIOSIDE G_{M1} AND β -C INTEGRIN ARE LOCALIZED TO THE APICAL PLASMA MEMBRANE IN CLEAVAGE STAGE EMBRYOS.....	26
FIGURE 2: POLARITY PROTEINS PAR6 AND CDC42 LOCALIZE TO THE APICAL PLASMA MEMBRANE IN CLEAVAGE STAGE EMBRYOS, IN CONTRAST TO APKC	28
FIGURE 3: POLARIZED PLASMA MEMBRANE DOMAINS ARE STABLE IN DISSOCIATED BLASTOMERES	30
FIGURE 4: G_{M1} LOCALIZATION TO THE APICAL CELL SURFACE IS INDEPENDENT OF ACTIN AND ACTOMYOSIN CONTRACTION, BUT DEPENDENT ON MYOSIN FILAMENT ASSEMBLY	32
FIGURE 5: PAR6 APICAL LOCALIZATION IS DEPENDENT ON CALCIUM-MEDIATED CELL ADHESION, ACTIN, AND APKC ACTIVITY	34
FIGURE 6: ENDOCYTOSIS IS POLARIZED TO THE G_{M1} RICH APICAL CELL SURFACE	36
FIGURE 7: FUNCTIONAL APKC IS REQUIRED FOR NORMAL CLEAVAGE PLANE DETERMINATION AND BLASTULA FORMATION.....	38
FIGURE 1-2: GANGLIOSIDE G_{M1} RECOVERS TO THE BLEACH REGION OF INTEREST AT MID-ANAPHASE.	58
FIGURE 2-2: FLUORESCENCE INTENSITY INCREASE GREATER THAN 40% TO THE BLEACHED ROI IS DESIGNATED AS RECOVERY	60
FIGURE 3-2: GANGLIOSIDE G_{M1} POLARIZED TO THE APICAL MEMBRANE CORTEX IN DISSOCIATED BLASTOMERES MIGRATES INTO THE BASOLATERAL FURROW AND SUBSEQUENTLY CLEARS	62
FIGURE 4-2: MYOSIN FILAMENTS PLAY A LARGER ROLE IN G_{M1} SCAFFOLDING THAN MICROTUBULES OR ACTIN	64
FIGURE 5-2: DISSOCIATION OF BLASTOMERES INCREASES G_{M1} MOBILITY IN THE MEMBRANE CORTEX	66
FIGURE 6-2: MYOSIN LOCALIZATION CHANGES UPON DISSOCIATION OF 2 AND 4 CELL STATE EMBRYOS	68-70
FIGURE 7-2: INHIBITION OF MYOSIN LIGHT CHAIN KINASE DISRUPTS PAR6, APKC, AND Cdc42 APICAL LOCALIZATION	72
TABLE 1: MYOSIN FILAMENTS PLAY A LARGER ROLE IN G_{M1} SCAFFOLDING THAN MICROTUBULES OR ACTIN	74
TABLE 2: DISSOCIATION OF BLASTOMERES INCREASES G_{M1} MOBILITY PRIOR TO ANAPHASE.....	75

Chapter 1: Introduction

Introduction

Polarized distribution of different cellular components is a fundamental concept in development. It is also a requirement for several functions on the cellular level including asymmetrical cell division, cell migration, and spindle positioning. Therefore, polarity is categorized into three different types: embryonic, cellular, and planar. Embryonic polarity has been studied most thoroughly in the protostomes *Caenorhabditis elegans* and *Drosophila melanogaster*. Providing two contrasting ways to form an early embryo, *C. elegans* and *Drosophila* are very suitable systems for genetic manipulation and analysis. Despite not being a genetic model system, the sea urchin embryo has been a model for developmental biology for over a century. The sea urchin, an echinoderm, is most closely related to vertebrates phylogenetically, including its deuterostome development. Hence, it is an attractive model system with a development resembling our own. Here, I use the knowledge of embryonic polarity we have gained from *C. elegans*, *Drosophila*, and other model organisms with that of sea urchin development to address the question of polarity in cleavage stage sea urchin embryos. Since asymmetry of daughter cell size begins at the fourth cell division, thus in addition to embryonic polarity, cell polarity of early blastomeres has also been studied.

Our knowledge of cell polarity comes mostly from the study of epithelial and migrating cell types (Conti and Adelstein, 2008; Li and Gundersen, 2008). Trafficking, directional targeting, and asymmetries of the cell have also been examined in *Drosophila* neuroblasts, polarized epithelial cells, mammalian neurons, and yeast. The same

determinants thought to be responsible for embryonic polarity are highly conserved and play a role in cell polarity as well. The PAR complex, consisting of PAR6, atypical protein kinase C (aPKC), and PAR3, was first discovered in the Kemphues lab in 1995 while studying *C. elegans* embryonic polarity and is the key player in cellular and embryonic polarity. The mechanisms found responsible for the establishment and maintenance of cell polarity were the basis for my investigation into the regulation of polarity in the sea urchin embryo. Interactions of polarity determinants, the dynamic cytoskeleton, and the cell cycle were each closely examined for their role in deuterostome early polarity.

Lastly, study of planar polarity has been emerging with the investigation of tissue morphogenesis (Tanentzapf and Tepass 2003). Planar cell polarity studies have confirmed a conserved role for the PAR complex of proteins, the same ones involved in embryonic and cell polarity. Examples of planar cell polarity in sea urchin development include invagination at the vegetal plate during gastrulation and the formation of the long tuft of cilia on the apical ectoderm. As researchers continue to investigate embryonic, cell, and planar polarity in model systems, the PAR complex has been consistently implicated. Polarity of the cleavage stage sea urchin embryo, a model deuterostome, is studied here for the first time.

Background

Embryonic, Planar Cell, and Cell Polarity

One type of embryonic polarity is anteroposterior, which has been studied in depth in *C. elegans* and *Drosophila* embryos (Doe, 2001; Suzuki and Ohno, 2006). The

highly conserved complex of polarity proteins, the PAR complex, founded in *C. elegans*, has been the focus of embryonic polarity research since Kemphues and colleagues cloned two of the six partitioning-defective genes, PAR-1 and PAR-3 (Guo and Kemphues, 1995). In the last 10 years, scientists have refined the mechanism maintaining PAR polarity determinants at particular cortical locations in a number of cell types (Henrique and Schweisguth, 2003). The PAR-aPKC (atypical protein kinase C) system consists of three determinants polarized to the apical, anterior, or leading edge: two PDZ-domain-containing scaffold proteins, PAR-3 and PAR-6, and the serine/threonine protein kinase, atypical protein kinase C (aPKC). Opposing these are three basal, posterior, or rear end polarity determinants: PAR-1, PAR-4, and PAR-2. Although the specific mechanism by which the PAR proteins direct global polarization of cells varies depending on cell type, the opposing interactions of the PAR proteins at each cell end is evolutionarily conserved. In addition, Cdc42, a small GTPase, links the complex of PAR-6, PAR-3, and aPKC to the apical/anterior cortex (Garrard et al., 2003; Gotta et al., 2001; Hutterer et al., 2004; Qiu et al., 2000; Takahashi and Pryciak, 2007). Most recently, Nakayama et al. (2009) identified a role for dynamin in the polarity along the anterior-posterior axis of *C. elegans* embryos. Fluorescence imaging and knockdown of dynamin and the anterior polarity cues, PAR-6 and PAR-3, demonstrate their participation in plasma membrane dynamics and, subsequently, polarity maintenance.

Since microfilaments are involved in asymmetric embryonic patterning (Hill and Strome, 1988, 1990), Kay and Hunter examined Cdc42, an actin cytoskeleton regulator, for its role in PAR protein localization (2001). Knockdown of Cdc42 disrupted the asymmetric localization of the PAR complex and this was confirmed upon closer

examination of the acto-myosin cytoskeleton by Cowan and Hyman (2007). Along with Jenkins et al. (2006), they found reorganization of the acto-myosin cortex, initiated by sperm centrosomes and the RhoGAP CYK-4, resulted in contractile asymmetry in *C. elegans* embryos. An actomyosin gradient is created along the embryo and Cdc42, in concert with Rho-GTPase, mediates the differential recruitment of PAR polarity determinants to the anterior of the embryo. Furthermore, another RhoGAP, PAC-1, was identified at cell contacts in early *C. elegans* embryos as excluding active Cdc42 (Anderson et al., 2008). With active Cdc42 at contact-free cell surfaces, PAR-6 can then be recruited and polarized.

Guo and Kemphues had found that mutations in the nonmuscle myosin heavy chain II (NMY-2) disrupted embryonic polarity and asymmetric division in *C. elegans* embryos (1996). NMY-2 binds PAR-1, a polarity determinant localized to the posterior of wild-type embryos. Disruption of this interaction affects the localization of PAR-1, PAR-2, also localized to the posterior, and PAR-3, normally localized to the anterior along with PAR-6 and aPKC (Severson and Bowerman, 2003). In addition, RNA-mediated genetic interference of *nmy-2* or *mlc-4*, a conserved nonmuscle myosin II regulatory light chain, disrupts anterior-posterior polarity, possibly by interference with polarized cytoplasmic flow (Shelton et al., 1999). Schonegg and Hyman (2006) found the GTPases CDC-42 and RHO-1 to coordinate the asymmetric contractility of the acto-myosin network at fertilization with PAR protein localization (Schonegg et al., 2007).

Polarity has also been studied in vertebrate embryos, but most of the work focuses on cell morphogenesis and organogenesis, which involves planar cell polarity. Though their function is largely unknown in *Xenopus*, aPKC, ASIP/PAR-3, and PAR-6 localize

to the animal pole during oocyte maturation (Nakaya et al., 2000; Choi et al., 2000). Atypical protein kinase C (aPKC) is also involved in convergent extension during *Xenopus* gastrulation with PAR-6, cell fate determination in the epidermis with PAR-1, and polarity of neuroepithelial progenitor cells (Hyodo-Miura et al., 2006; Ossipova et al., 2007, 2009). ASIP/PAR-3 and protein kinase C, iota (PrkCi, a member of the Par complex) are apically localized in zebrafish neuroepithelial cells and spinal cord precursors, respectively (von Trotha et al., 2006; Roberts and Appel, 2009). In addition, PrkCi is required for asymmetric planar divisions in renewing precursor cells (Roberts and Appel, 2009).

Similar work has been performed in mouse models (Sapir et al., 2008; Atwood et al. 2007), and Vinot et al. (2005) demonstrated polarity establishment in the early mammalian embryo. The homologue of PAR-6, PARD6b, is polarized as early as the 8-cell stage after compaction (Vinot et al., 2005). Prior to this, from the 2-cell stage to the 8-cell stage, PARD6b is both nuclear and distributed within the cytoplasm suggesting it is not active since it is not associated with the membrane cortex. Following compaction, PARD6b localizes to the apical pole of the polarized cells. The lack of work on early deuterostome embryonic polarity lends itself to the need for careful study of a model deuterostome.

The dynamic between the PAR proteins and their interactors has a conserved role in cell polarity as well. Cell polarity has been extensively studied in epithelial, migrating, and neuronal cells (Martin-Belmonte and Mostov, 2008; Schuck and Simons, 2004). Epithelial cells demonstrate apical-basolateral polarity where the apical cell surface faces the lumen of the organ and the basolateral surface faces the submucosa. One feature

unique to epithelial cells is the presence of physical junctions separating the polarized regions. At the apical cell surface, the PAR complex, PAR6, PAR3, and aPKC, is present while PAR-1 and PAR-2 oppose this localization (Li and Gundersen, 2008). The cytoskeleton, PAR determinants, and additional cell machinery such as vesicle trafficking respond to polarity signals and structures within the cell. Migrating cells, in contrast, respond to external cues that direct polarity within the cell. The inherent structure of the neuron, with a cell body, axon, and dendrites, favors cell polarity. Cells responsible for the directional transmission of signals in mammals also possess the conserved PAR polarity proteins. The stable polarized microtubules of the neuron have a high amount of acetylated tubulin in the axons compared to undifferentiated neurites. Kinases including PAR1 and aPKC have been implicated in tubulin stability (Dotti et al., 1991; de Anda et al., 2005).

Polarity during Early Echinoderm Development

Horstadius is a name that commonly arises in reference to sea urchin development. His early experiments, around 1973, detailed embryonic polarity along the animal-vegetal axis through transplantation and blastomere isolation experiments. Most notably, Horstadius (1973) transplanted the micromeres of the vegetal half to the animal region of a 60-cell stage sea urchin embryo, which formed a secondary gut. This is evidence of planar cell polarity as the micromeres induce invagination of the animal half, but identification of PAR polarity determinants was about 25 years away. However, Sherwood and McClay (1997) did later identify the transcription factor, β -catenin, responsible for specifying the micromeres.

Embryonic polarity along the animal-vegetal axis has been the focus of developmental biologists studying echinoderms such as sea urchins, sand dollars, and starfish. At the fourth cleavage cell differentiation is initiated when the vegetal blastomeres unequally divide resulting in micromeres, precursors of the skeletogenic mesenchyme, and macromeres (Okazaki, 1975; Dan, 1960). Observations have been made of individual blastomere polarity in early echinoderm embryos. For example, Kuraishi and Osamai noted Nile blue-stained granules and microvilli distribution concentrated at the apical region, or the cell surface facing the exterior in 2 and 4 cell stage starfish embryos (1989). Likewise, Inoue noted the accumulation of pigment granules in dividing *Arbacia* sea urchin zygotes in the furrow, which cleared out after cleavage (1990). Prior to fertilization, these pigment granules are cytosolic and migrate to the cell cortex upon fertilization (Inoue, 1990). Granule and microvilli polarity was identified as functional in its requirement for embryonic integration (Kuraishi and Osamai, 1989). Reoriented starfish blastomeres within their fertilization envelopes failed to successfully form blastulae. This is partially due to that fact that the basal cortex, which Kuraishi and Osamai termed the Nile blue-stained granule-free region, acquires adhesiveness during blastulation that the apical cell cortex does not.

Similarly, Schroeder characterized apically localized pigment granules and microvilli (1988) soon after McCaig and Robinson observed lectin receptors, stained with wheat germ agglutinin, at the apical surface of early sea urchin blastomeres (1982). Schroeder noted the pigment granules and microvilli coordinately faced the hyaline layer and were absent from the basolateral surfaces of adjacent blastomeres. He also observed, upon dissociation, that the blastomeres maintained these polarized structures. Thus, sea

urchin blastomeres have a self-polarizing capacity, which is not dependent on extracellular/intracellular signals or cell contact. In fact, junctions and physical attachments are not yet present between blastomeres (Spiegel and Howard, 1983). Croce and McClay (2006) noted the concentration of *disheveled*, an upstream regulator of β -catenin in the canonical Wnt pathway, in the vegetal pole of fertilized zygotes and early cleaving embryos, the first indication of a real molecular polarity to this deuterostome egg as it is required for animal-vegetal axis patterning.

Miller and McClay (1997) published data suggesting the abundance of β -catenin and cadherin at cell-cell contacts between blastomeres of 2 and 4 cell stage sea urchin embryos. However, the slightly increased concentration to contact sites could be a result of overlapping plasma membranes. To date, there exists no evidence of PAR polarity determinant function in sea urchin embryos, though they are clearly predicted to play a role. Three Par-related genes were recently isolated from the sea urchin *Hemicentrotus pulcherrimus*: *Par-1*, *Par-6*, and *aPKC* (Shiomi and Yamaguchi, 2008). Thus, investigation into the mechanisms of control for cell polarity in cleavage stage sea urchin embryos is of interest.

Specific Aims

Specific Aim 1: To characterize cell polarity in cleavage stage sea urchin embryos and identify the mechanisms of its establishment.

Specific Aim 2: To determine the spatial and temporal regulation of membrane cortex asymmetry in early sea urchin embryos.

Chapter 2: Cell Polarity Emerges at First Cleavage in Sea Urchin Embryos

Introduction

Asymmetrically localized information laid down during oogenesis determines the early axis and specifies cell fate, as initially studied in protostomes. *C. elegans* embryos have a highly polarized cortex and localized determinants, leading to determinative development. The molecular nature of this early polarity is defined by the Par polarity complex, composed of two PDZ domain containing adaptor proteins, PAR6 and PAR3, working in concert with atypical protein kinase C (aPKC) and the GTPase Cdc42. The egg shows differential localization of PAR proteins at fertilization into the anterior-posterior axis, thus segregating determinants at the first cell division (Cowan and Hyman, 2004; Doe and Bowerman, 2001; Munro, 2006; Severson and Bowerman, 2003). Polarity in *C. elegans* embryos, established at fertilization, is initiated and maintained by the actomyosin cortex that restricts the PAR6 complex to the anterior domain (Cowan and Hyman, 2007; Munro, 2006). The PAR proteins play a conserved role of controlling asymmetric divisions in worms, flies, frogs, and mammals and likewise plays a similar role later in development in asymmetric divisions in mature epithelial cells (Chalmers et al., 2003; Macara, 2004; Muller and Hausen, 1995; Ohno, 2001; Plusa et al., 2005; Suzuki and Ohno, 2006; Vinot et al., 2005). However, the roles of the PAR complex in the initial stages of deuterostome development, including the chordata and echinoderms, remains less well characterized.

Some deuterostome eggs do show cortical polarity or developmental restrictions, such as along the animal-vegetal axis. For instance, localization of the Wnt pathway signaling protein Disheveled localizes to the vegetal pole occurs in echinoderms (Croce and McClay, 2006) likely reflecting the inability of the animal half of a fertilized egg to develop normally (Horstadius, 1973). In mammals, the asymmetric localization of Par proteins or of aPKC in the embryo does not appear until at least the 8 to 16 cell stage when they are found at the apical pole of the polarizing blastomeres (Plusa et al., 2005; Vinot et al., 2005). In amphibian eggs, meiotic maturation induces asymmetric localization of aPKC and Par3 to the animal hemisphere. (Nakaya et al., 2000). Cell polarity is next seen at the 64 cell stage, when blastomeres of the *Xenopus* embryo are autonomously polarized with aPKC localized to the apical or free cell surface (Muller and Hausen, 1995). During formation of the first epithelium in amphibian embryos, aPKC is polarized to the apical domain and directs the formation of the superficial cells of the developing blastula (Chalmers et al., 2003). Likewise, ascidian embryos are very determinative in development and Patalano et al. (Patalano et al., 2006) have found polarity in the ascidian egg cortex with the PAR complex localized to the centrosome attracting body during asymmetric divisions, which begin at the 8 cell stage.

Early cleavage divisions also give rise to epithelia with apical-basolateral polarity. Interestingly, the same Par polarity complex proteins play integral roles in the establishment of apical-basolateral polarity in development (Martin-Belmonte and Mostov, 2008). Cell polarity can also be established through membrane trafficking in early cleavage. Essential for the completion of cytokinesis (Albertson et al., 2005; D'Souza-Schorey and Chavrier, 2006; Finger and White, 2002), the membrane inserted

into the late furrow is likely to possess unique properties. For instance, in amphibian embryos, membrane inserted into the furrow possesses the cell adhesion molecule β 1-integrin (Gawantka et al., 1992) and thus early apical-basolateral cell surfaces are established. Membrane trafficking occurs late in the cleavage furrow to provide the added membrane surface area required in such embryonic cells as those from sea urchins (Conner and Wessel, 1999; Shuster and Burgess, 2002), *Drosophila* (Burgess et al., 1997; Hickson et al., 2003; Lecuit and Wieschaus, 2000; Riggs et al., 2003; Sisson et al., 2000), *C. elegans* (Bowerman and Severson, 1999; Jantsch-Plunger and Glotzer, 1999; Skop et al., 2001), zebrafish (Feng et al., 2002), and amphibians (Bluemink and de Laat, 1973; Byers and Armstrong, 1986; Danilchik et al., 2003; Danilchik et al., 1998). Associated with this trafficked plasma membrane are key signaling molecules including Rho, lipid signaling molecules and kinases (Bement, 2007; Bement et al., 2005; Ng et al., 2005; Piekny et al., 2005; Skop et al., 2004). As a result, new membrane insertion into the furrow provides distinct membrane proteins and lipids. In cleaving large amphibian embryos, this new membrane in the furrow provides the basolateral surface of the future blastula.

In this report, we find that the new membrane delivered in the cleavage furrow of the sea urchin zygote provides for a distinct apical and basolateral surface at the first division. The Par complex, found to be polarized in cellular localization at the first cell division, is also shown to play a key role in cleavage plane determination, in organization of the embryo, and in normal blastula formation. Further, we find that early blastomeres are functionally polarized by restricting actin-dependent endocytosis to only the apical cell surface. These results support that, like protostomes and larger deuterostome eggs,

sea urchin embryos exhibit early embryonic and cellular apical-basolateral functional polarity and this polarity is controlled by the Par complex.

Results

Cell Surface and Cortical Markers Are Polarized by Cytokinesis and Retained on the Former Egg Membrane.

Cleavage divisions result in the transformation of a seemingly unpolarized egg membrane to a polarized epithelium of a blastula that has both an apical surface facing the outside and a basolateral surface facing the inside. In most embryos, establishment and maintenance of the apical membrane distinct from the basolateral membrane is due to formation of tight junctions after the third through the fifth cleavage division (Fleming et al., 2000). Previously we found that ganglioside G_{M1} , which is evenly distributed in fertilized eggs, migrates and concentrates in the cleavage furrow with lipid rafts during early cytokinesis of the first cell division in sea urchin embryos (Ng et al., 2005). To observe ganglioside G_{M1} , embryos were pulse labeled with Alexa 488 cholera toxin B (CTB) during interphase of the first cell cycle and observed during the first cell division by confocal timelapse microscopy. Following the completion of cytokinesis, in the furrow area where ganglioside G_{M1} had concentrated, the CTB labeled membrane appeared to be pushed out of the area of the former cleavage furrow, leaving the plasma membranes in the interface between the two blastomeres unlabeled (Fig. 1a, supplemental movie 1 (online at Developmental Biology: doi: 10.1016/j.ydbio.2009.02.039)). This is seen more dramatically after the second cleavage division when ganglioside G_{M1} is localized solely to the outer, or free, cell surface (Fig.

1b, supplemental movie 2 (online at Developmental Biology: doi:10.1016/j.ydbio.2009.02.039)). These results are consistent with the wide-spread findings in animal cell cytokinesis that new membrane is inserted into the late cleavage furrow, something we noted in cleaving sea urchin blastomeres (Shuster and Burgess, 2002).

One sign of precocious cell polarity at the two and four cell stages in echinoderm embryos is the fertilization-induced elongation of actin rich microvilli. We find that the apical plasma membrane surfaces, rich in microvilli and facing the outside of the embryo, were labeled with CTB whereas basolateral inner plasma membrane surfaces, generally microvillus free, were not labeled. They are retained only on the blastomere surface facing the extracellular matrix, even when the blastomeres are dissociated, whereas the surfaces facing the future blastocoel are relatively bare of microvilli (Schroeder, 1988). Likely reflecting this polarized distribution of microvilli is the distribution of the $\alpha\text{B}\beta\text{C}$ subunits of integrins (Burke et al., 2004). Interestingly, $\alpha\text{B}\beta\text{C}$ integrins are found to be present only on the outer surface exposed to the extracellular matrix as early as the two cell stage (Burke et al., 2004). Using the anti-integrin antibody from these studies, we found that the localization of integrins corresponded exactly to surfaces labeled with 488 CTB in fixed, immunostained 2 and 4 cell stage embryos (Fig. 1c). Integrins were not present on the blastomere-to-blastomere contacting membranes.

The fixation protocol does not allow for co-localization of PAR6, Cdc42 or aPKC at the same time as G_{M1} , however, similar localization patterns of PAR6 and Cdc42 to ganglioside G_{M1} were seen in fixed, immunostained 2 and 4 cell stage embryos (Fig. 2a,b). We found that PAR6 and Cdc42 were excluded from the contact sites between

blastomeres. The localization pattern of aPKC, using an antibody which detects both the active and inactive forms, differed from that of both the ganglioside G_{M1} and PAR6 as shown in fixed, immunostained embryos. Enriched at the cleavage furrow during cytokinesis (Fig. 2c), aPKC then spread throughout the entire cell cortex after division had completed (Fig. 2d). Thus, inactive and/or active aPKC, in contrast to G_{M1}, integrins, PAR6, and Cdc42, does not appear to be apically localized in early echinoderm development.

Polarized Plasma Membrane Domains are Independent of Ca²⁺- dependent Cell Adhesion and Actin but Dependent on Myosin Filament Assembly.

To test whether the polarity of ganglioside G_{M1} enriched membranes was dependent on Ca²⁺-dependent cell adhesion, embryos that had been pulse labeled with 488 CTB in interphase of the first cell cycle were dissociated at the beginning of the 4 cell stage in calcium free sea water and then observed by confocal timelapse microscopy. The polarized membrane domains remained in the dissociated blastomeres, and live cell imaging showed the extent of CTB labeled membrane remained constant through the next cell cycle (Fig 3a). In a reciprocal experiment, unlabeled embryos were dissociated at the beginning of the 4 cell stage, and the dissociated blastomeres were then labeled with CTB and followed by confocal timelapse microscopy. CTB-labeled membrane was detected only over the microvillus-bearing (apical) surface and also was found to be stable throughout the next cell cycle. When dissociated two or four cell embryos were fixed and immunostained for integrins and labeled with CTB, it was found that the dissociated blastomere surfaces were polarized with coincident integrin and CTB staining (Fig. 3a).

Although the hyaline layer, an extracellular secreted calcium-dependent adhesion material, does not enter the interface between cells, hyalin is not responsible for this polarity. The embryos stained with CTB were often raised in calcium free sea water to allow for ease of dissociation. Without calcium, hyalin solubilizes and is thus removed from the extracellular matrix (Kane, 1973). In addition, many washes with calcium free sea water did not remove or alter the localization of G_{M1} .

In order to determine whether the actin cytoskeleton is required for maintaining polarized membrane domains, dissociated live four-cell stage blastomeres labeled with CTB were treated with cytochalasin D to disrupt the actin cytoskeleton while the cells were imaged by timelapse confocal microscopy. Following treatment with cytochalasin D, ganglioside G_{M1} remained in its original polarized distribution (Fig. 4d'). These cells became bi-nucleate confirming that actin filaments of the contractile ring were disrupted but that the normal mitotic cycle continued (Fig. 4d).

Non-muscle myosin II provides the motor force for cytokinesis and is present throughout the egg cell cortex (Lucero et al., 2006; Walker, 1994). ML-7, an inhibitor of myosin light chain kinase (MLCK) activity, prevents myosin assembly and has been shown to block assembly of the contractile ring whereas blebbistatin, which blocks myosin's ATPase activity, does not inhibit ring assembly but does block ring contraction (Murthy and Wadsworth, 2005). We found that ML-7 causes redistribution of ganglioside G_{M1} around the entire cell surface of dissociated live 4 cell stage blastomeres (Fig. 4f') whereas blebbistatin had no effect on ganglioside G_{M1} apical distribution (Fig. 4e'). Thus, myosin assembly into bipolar filaments likely plays a role in membrane polarity.

Membrane Lipids Are Segregated by Cleavage and Remain Distinct After Membrane Manipulation.

To visualize the nature of non-raft plasma membrane lipid domains, the fluorescent diunsaturated long chain hydrocarbon *FAST* DiI, which is excluded from domains of the plasma membrane rich in cholesterol, was used to label dissociated 4 cell stage blastomeres. With a micromanipulator, an oil droplet saturated with *FAST* DiI was touched to the plasma membrane on the 488 CTB free zone and the spreading of *FAST* DiI labeled membrane was followed by confocal timelapse microscopy. *FAST* DiI initially spread very quickly through the CTB free membrane zone but then became restricted when it reached the boundaries of the CTB labeled area and did not spread (Fig. 3b). In a complimentary experiment, the CTB free zone was labeled with the saturated long chain hydrocarbon DiI_{C18}, which is able to diffuse into raft plasma membrane domains. It was found that DiI_{C18} was able to diffuse throughout the entire plasma membrane and was not restricted to the CTB free zone (Fig. 3c, Supplemental movie 3 (online at Developmental Biology: doi: 10.1016/j.ydbio.2009.02.039)).

Manipulation of individual blastomeres demonstrated that this segregation of cholesterol-rich membrane domains is a reflection of established polarity. Sea urchin embryos are excellent at healing after membrane wounding. The apical surface of a four cell stage embryo was labeled with 488 CTB, the blastomeres were dissociated in calcium free sea water and resuspended in sea water. Using a microneedle, the non-CTB labeled membrane was cut and removed from the blastomere, leaving a nucleated apical-only cell (Fig. 3d). This apical-only cell subsequently divided and inserted new

ganglioside free membrane in the furrow. By adding a second color fluorescent CTB, the new membrane is shown to not contain any ganglioside G_{M1} (Fig. 3d, overlay). Thus, the lipid domains, gangliosides, integrins, and the Par complex are all separated into apical or basolateral domains by early cleavage divisions.

Ca²⁺ - mediated Cell Adhesion, the Actin Cytoskeleton, and Functional aPKC Are Required for PAR6 Localization.

Dissociated two and four cell stage embryos, generated by washing embryos in calcium free sea water, were fixed and immunostained for PAR6 revealing that PAR6 lost its polarity to the apical cell surface (Fig 5a'). We found that as soon as 15 minutes after dissociation, PAR6 re-localized to the entire cell surface of the isolated blastomeres. Thus, in contrast to ganglioside G_{M1} localization, PAR6 polarization is dependent on Ca²⁺-dependent cell adhesion.

We also were interested in the dependency of PAR6 on an intact actin cytoskeleton. We treated intact, adherent 2 cell stage embryos with cytochalasin D for 15 minutes, then fixed and immunostained for PAR6. PAR6 localization had not only redistributed to the entire cell surface, but also became cytoplasmic (Fig. 5b). Upon washout of cytochalasin D, PAR6 re-localized to the free apical cortex and was excluded from the cell-cell contact surfaces (Fig 5c). In contrast to ganglioside G_{M1} localization, PAR6 apical localization depends on actin filaments.

The interaction of PAR6 and aPKC has been shown to be essential for the function of the aPKC polarity complex. Using an antibody against aPKC for co-immunoprecipitation followed by using a PAR6 antibody for western blotting, we

confirmed a complex of aPKC and PAR6 exists in sea urchin embryos (Fig. 5f). Lysate from 2 cell stage embryos, in which Par polarity is first detected, was used for co-immunoprecipitation. Subsequently, we used a myristolated PKC-zeta cell permeable peptide inhibitor to specifically inhibit aPKC (Ward and O'Brian, 1993; Zhou et al., 1997), thereby determining the dependency of PAR6 and the ganglioside G_{M1} polarized localization on a functional aPKC complex. Live embryos at the 2 cell stage, labeled with 488 CTB, were treated with the inhibitor and imaged by confocal microscopy. The apical membrane localization of the ganglioside G_{M1} was not affected by treatment with the aPKC inhibitor (Fig. 5e). To examine the effects of aPKC inhibition on PAR6 localization, 2 cell stage embryos were treated with the aPKC inhibitor for 15 minutes, then fixed and immunostained for PAR6. In contrast to the ganglioside G_{M1} , PAR6 redistributed around the entire cell cortex and became cytoplasmic in these embryos, illustrating that its polarized localization is dependent on a functional aPKC polarity complex (Fig. 5d). The effect of the aPKC inhibitor on PAR6 localization was fully reversible upon washout (data not shown).

Functional Polarity Exists at the Early Cleavage Stages.

a. Endocytosis is Polarized in Cleavage Blastomeres.

Fluorescent dextran molecules have been used to follow compensatory endocytosis after fertilization in sea urchin eggs (Whalley et al., 1995) and we used this method to determine sites of endocytosis in cleavage stage embryos. Dissociated two, four, or eight cell stage embryos were labeled with 488 CTB to identify the apical surface and then pulsed with fluorescent dextran for 10 minutes (Fig. 6). Timelapse imaging

shows that endocytosis occurs selectively on the G_{M1} rich apical surface in cells from all blastomeres tested (Fig. 6d). Thus, there is functional polarity established in the first cleavage divisions. Cytochalasin D treatment to disrupt actin filaments abolished dextran endocytosis whereas nocodazole treatment to disrupt microtubules did not effect initial endocytosis but the vesicles did not migrate beyond the cell cortex (data not shown). Additionally, aPKC inhibition in dissociated blastomeres does not disrupt endocytosis or the polarity of the endocytosed vesicles (data not shown).

b. The Par Complex Plays a Role in Normal Cleavage Plane Determination and Development.

Sea urchin eggs undergo stereotypical cleavage divisions; for instance, the third cleavage results in two tiers of four blastomeres. Inhibition of aPKC at the 4 cell stage does not block cell division but results in 91.7% (42 of 46 observed) of the 8 cell embryos with cleavage plane defects (Fig 7c,d). Examination of the mitotic apparatus microtubules by immunofluorescence reveals a number of spindle orientation and spindle defects (Fig. 7a,b), which result in the organization of all 8 blastomeres in the same plane and birth of unequal sized cells (Fig. 7c,d). Two cell stage embryos treated with aPKC inhibitor resulted in cells with multiple spindles, cells with eccentrically placed spindles, multipolar spindles, and spindles with short asters (Fig. 7a,b). These spindle defects lead to the eventual apoptosis of embryos and the inability to develop into a blastula.

The effect of aPKC inhibition, using doses allowing for cleavage, on blastula formation is dependent upon the developmental stage at which the inhibitor was added. Consistently compromised in blastula formation, embryos treated at progressively later cleavage stages were more successful in forming blastula stage embryos (Fig. 7e). When

the aPKC zeta peptide inhibitor was added at the one, two, or four cell stages, embryos underwent one additional round of division, but subsequently apoptosed. Over 60% of embryos treated with the inhibitor at the 16 cell stage were able to form blastulae; however, the epithelium of these blastulae were highly compacted compared to the control (Fig. 7e, inset). In addition, these effects are reversible upon washout of the aPKC inhibitor after 15 minutes of treatment (data not shown). Thus as development proceeds, disruption of early polarity directed by the Par complex has a decreased effect on the ability of the embryo to form a blastula.

Discussion

The results in this study provide evidence that structural and functional cell polarity in sea urchin zygotes appears at the first cell division. We find that apical-basolateral cellular polarity is established at the first cell division by partitioning of the egg cortex and plasma membrane. The apical or outer cell surface remains distinct from the newly generated basolateral surface at the cell-cell contact site, much as has been shown in early cleaving amphibian zygotes. Using markers of the apical cell surface, of membrane domains, and of conserved polarity proteins, we find that new membrane insertion at the cleavage furrow provides basolateral membrane that remains distinct from the apical membrane. Heretofore, it has been suggested that most deuterostome embryos with the notable exceptions of amphibian and ascidian embryos do not exhibit cellular structural and functional polarity until the development of tight junctions between blastomeres in the early blastula stage, which provide for the barriers between apical and basolateral surfaces after the first three or four cell divisions (Fleming et al., 2000).

However, our findings suggest that true cellular polarity may exist in deuterostome embryos in general.

In a few embryos, including amphibians, tight junctions first form at the two cell stage although they may not assume their apical locations until much later (Cardellini et al., 1996; Chen et al., 1997; Fesenko et al., 2000; Merzdorf et al., 1998). However, sea urchin eggs do not assemble tight junctions until at least the eight cell stage (Andreuccetti et al., 1987; Spiegel and Howard, 1983). Interestingly, in sea urchin embryos, early reports suggested that isolated blastomeres from the first cleavage divisions are able to have a self polarizing capacity (Dan, 1954a; Dan, 1954b; Dan, 1960). The results reported here show that the Par complex, Ca^{2+} -dependent cell adhesion, and the actin cytoskeleton can serve the novel function in early cleaving blastomeres of establishing and maintaining the apical-basolateral cell polarity that is established at the first cell division in the absence of cell junctions.

The sea urchin egg membrane changes at fertilization with the exocytosis of membrane and the formation of thousands of microvilli due to actin filament assembly. Accompanying the morphological transformation of the egg surface is the appearance of unusual integrins which associate with the cortical actin cytoskeleton (Burke et al., 2004). In addition, we find that the Par complex, including PAR6, aPKC and Cdc42, are polarized after each cleavage division by being restricted to the apical cortical region of the blastomeres in an actin dependent manner. It appears that for this relatively average sized egg, like for much larger amphibian eggs (Muller and Hausen, 1995), the fertilized egg membrane becomes the apical cell membrane and the basolateral membrane surface originates via targeted exocytosis in the cleavage furrow. Our findings are consistent with

the report that at the blastula stage, specific cell surface antigens are localized to and are maintained at the apical cell surface, even in dissociated blastomeres, in an actin filament dependent manner (Nelson and McClay, 1988).

We find that this structural polarity is reflected by true functional polarity at the earliest cleavage divisions. Not only are microvilli restricted to the apical cell surface in dividing blastomeres, but we also find that this apical cell surface is functionally distinct from the basolateral cell surface as it is competent to support actin dependent fluid phase endocytosis. The insensitivity of polarized endocytosis to aPKC inhibition suggests that the competency of the apical cell surface to fluid phase endocytosis is independent of the Par complex.

However, the PAR complex also plays a key functional role in embryonic polarity in this model deuterostome. We find that the complex is important in mitotic spindle orientation essential for proper cleavage plane determination and for normal blastula formation. These results are consistent with early observations that the aPKC-PAR complex plays a key role in mitotic spindle orientation in dividing *C. elegans* embryos (Etemad-Moghadam et al., 1995). Proper cleavage plane determination, as controlled by the PAR complex, is thus key for creating the stereotypical blastomere orientations in 8, 16, 32, etc. cell stage embryos. Interference with the PAR complex by inhibiting aPKC results in significantly compromised blastula development and thus proper animal-vegetal polarity, an effect that we have found to be reversible.

While mammalian embryos do not reveal molecular polarity until after several cleavage divisions, a strong polarity is exhibited during oocyte maturation divisions. Par-3 has been shown to be associated with a cortical actin cap in the pole of the oocyte

where polar bodies are born and the intact actin cytoskeleton is required for maintenance of the asymmetric Par-3 localization (Duncan et al., 2005). Whereas deuterostomes in general are regulative in development, the early mammalian embryo does show distinct cell polarity where cleavage divisions may play a key role in segregating determinants (Zernicka-Goetz, 2005). Thus, the results in the present study indicate that deuterostomes also show functional cellular polarity at the first cleavage division and that the Par complex plays a key role in the establishment of this polarity.

Figure 1

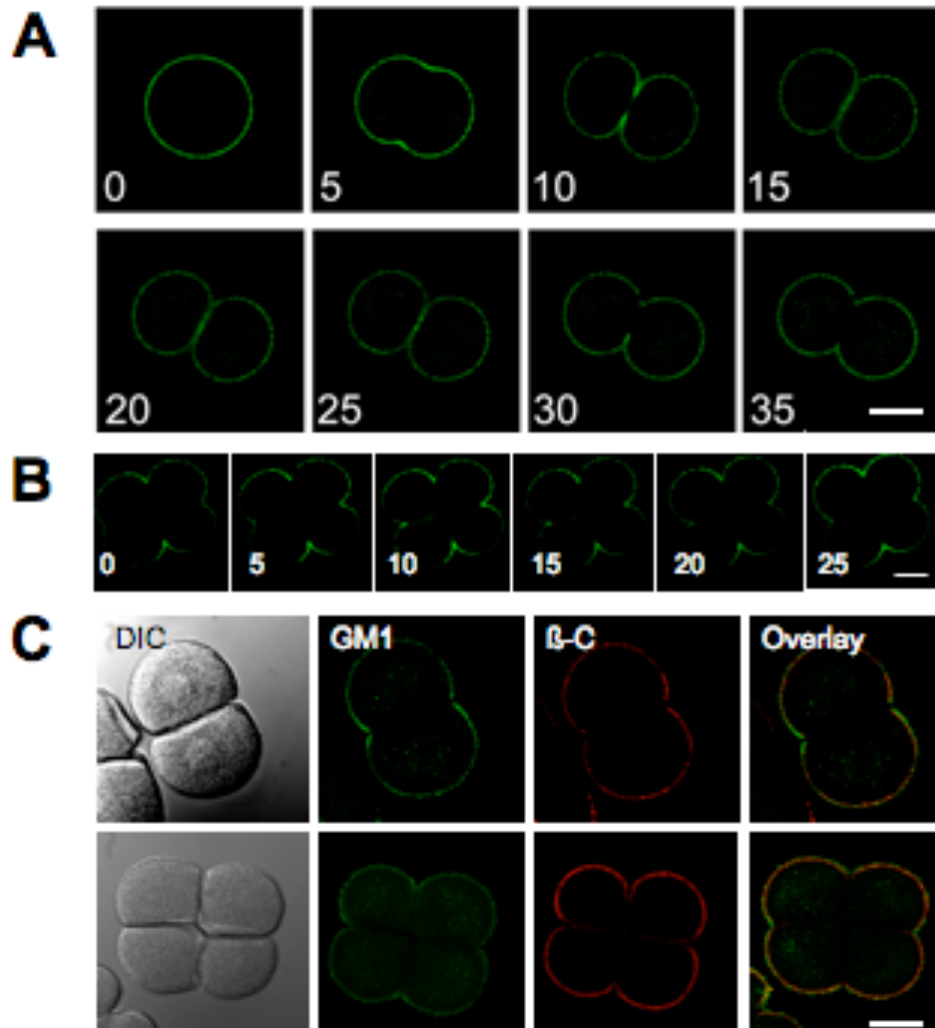


Figure 1: Ganglioside G_{M1} and β-C Integrin are localized to the apical plasma membrane in cleavage stage embryos. (A) The lipid raft marker, ganglioside G_{M1}, accumulates in the cleavage furrow at the first cell division, and it moves out of the interface between the blastomeres following the first cell division. Still images from a confocal timelapse movie of a live cell labeled with Alexa 488 CTB to visualize ganglioside G_{M1} (supplemental movie 1, online at Developmental Biology: doi: 10.1016/j.ydbio.2009.02.039). Time in minutes is indicated in the lower lefthand corner of each frame. Bar equals 50μm. (B) Ganglioside G_{M1} is localized to the apical outer plasma membrane surface in blastula stage embryos. Bar equals 50μm (C) Ganglioside G_{M1} and β-C integrin are localized to the apical plasma membrane in fixed, immunostained embryos. Confocal images of 2 and 4 cell stage embryos were labeled with alexa 488 CTB, then fixed and immunostained for β-C integrin. Bar equals 50 μm.

Figure 2

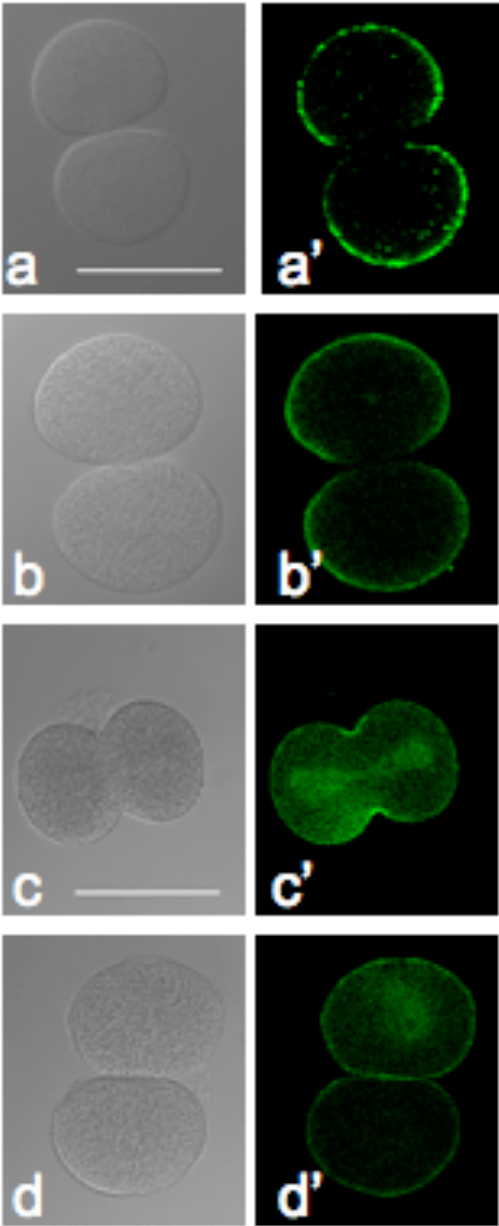


Figure 2: Polarity proteins PAR6 and CDC42 localize to the apical plasma membrane in cleavage stage embryos, in contrast to aPKC. PAR6 (a') and Cdc42 (b') both localize to the apical cortex in 2 cell stage embryos. Embryos were fixed and immunostained for PAR6 and Cdc42 and imaged using confocal microscopy. aPKC is enriched in the furrow during cleavage (c') and distributes around the entire cell cortex after the completion of division (d'). Embryos were fixed and immunostained for aPKC. Bar equals 75 μ m.

Figure 3

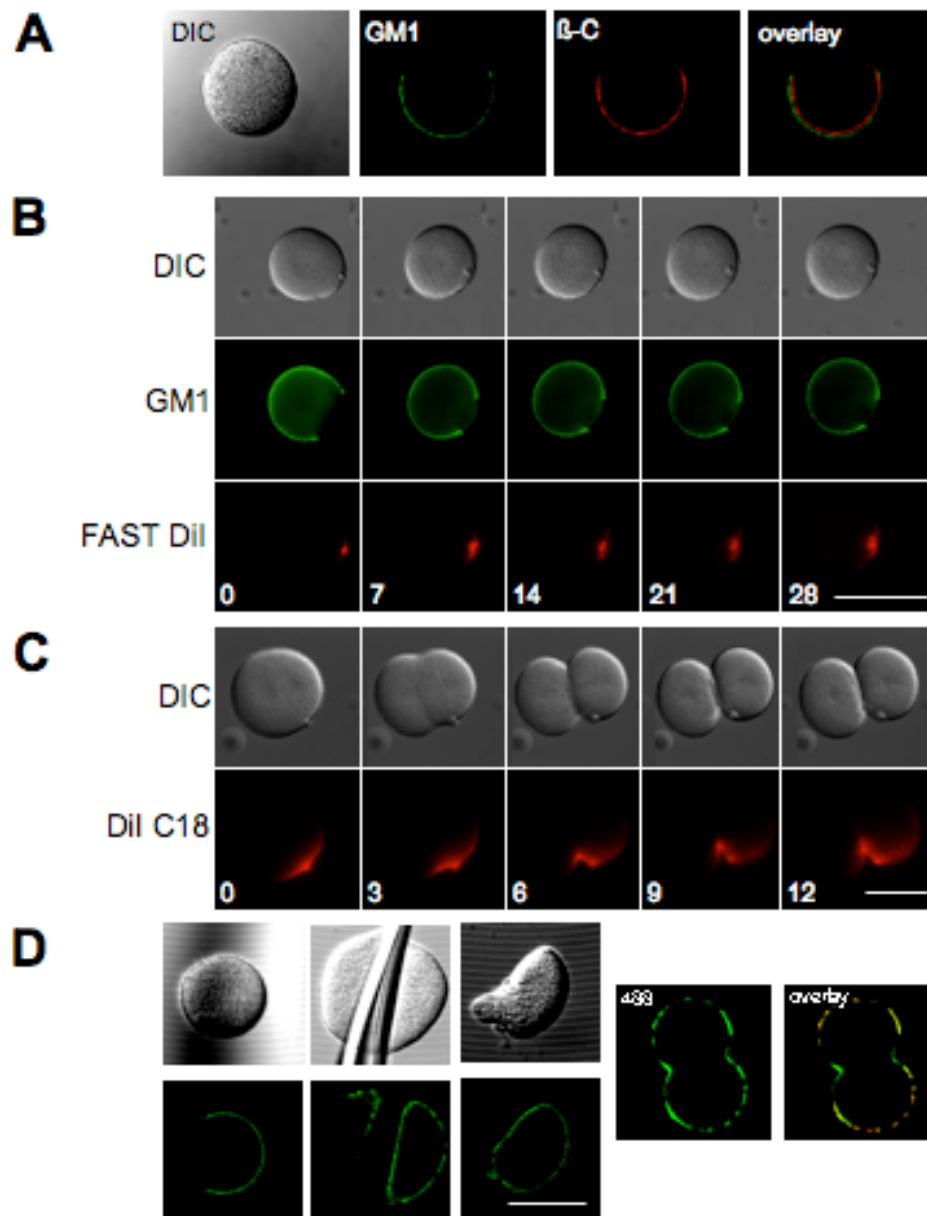


Figure 3: Polarized plasma membrane domains are stable in dissociated

blastomeres. (A) Ganglioside G_{M1} and β -C integrin remain localized to the apical cell surface of dissociated blastomeres. 4 cell stage embryos were first dissociated in calcium free seawater then stained with CTB prior to fixation and immunofluorescence. (B) The diunsaturated long chain dialkylcarbocyanine lipophilic tracer *FAST* DiI is restricted to the basolateral plasma membrane surface in dissociated blastomeres. A live dissociated four cell stage blastomere labeled with Alexa 488 CTB was co-labeled with an oil droplet saturated with *FAST* DiI. The *FAST* DiI initially spreads quickly throughout the ganglioside G_{M1} -free basolateral plasma membrane surface, but then is restricted to the basolateral plasma membrane. Time in minutes is indicated in the lower left hand corner of each frame. (C) A dividing zygote is touched with an oil droplet saturated with DiI C_{18} at the future cleavage furrow. The DiI C_{18} spreads laterally through the plasma membrane and also into the furrow of the dividing cell, where non-raft plasma membrane exists. Time in minutes is indicated in the lower left hand corner of each frame. (D) A glass microneedle, bent in the shape of a hockey stick, was used to cut and remove the non-CTB 488 labeled membrane from a dissociated blastomere,. The remaining nucleated apical-only cell subsequently divided and new non-raft membrane was added to the cleavage furrow of the manipulated blastomere. By adding a second color fluorescent CTB (555), the new membrane is confirmed to not contain any ganglioside G_{M1} . Bar equals 50 μ m.

Figure 4

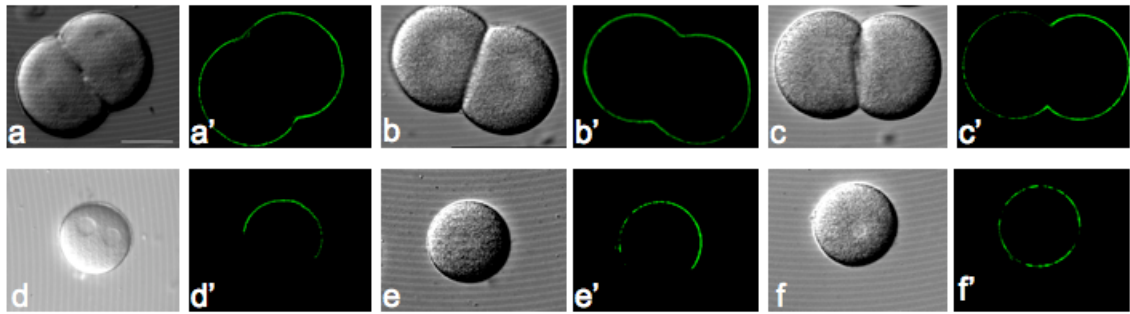


Figure 4: G_{MI} localization to the apical cell surface is independent of actin and actomyosin contraction, but dependent on myosin filament assembly. G_{MI} remains localized to the apical plasma membrane surface after treatment with cytochalasin D (10 μ M) (a'), blebbistatin (30 μ M) (b'), and ML-7 (100 μ M) (c') in 2 cell stage embryos. G_{MI} remains localized to the apical cell surface in dissociated blastomeres of 4 cell stage embryos treated with cytochalasin D (d') and blebbistatin (e'), but spreads around the entire cell cortex of those blastomeres treated with ML-7 (f'). Embryos were first stained with alexa 488 CTB then dissociated in calcium free seawater prior to drug treatments and imaging by spinning disk confocal microscopy. Bar equals 25 μ m.

Figure 5

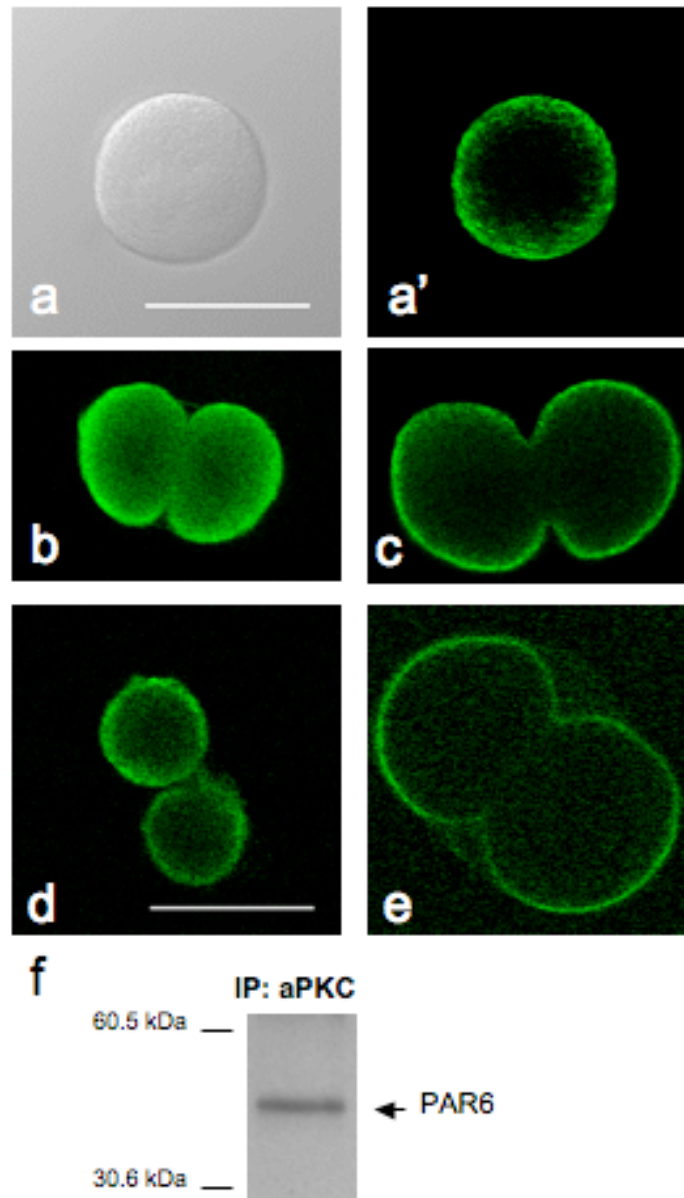


Figure 5: Par6 apical localization is dependent on calcium-mediated cell adhesion, actin, and aPKC activity. After dissociation of 4 cell stage embryos in calcium free seawater, Par6 redistributes around the entire cell cortex of individual blastomeres (a'). In 2 cell stage embryos, depolymerization of actin causes Par6 to lose its cortical localization (b). Embryos were treated with cytochalasin D (10 μ M) for 15 minutes then fixed and immunostained for Par6. This cortical disruption of Par6 is reversible upon washout of the drug (c). Embryos treated for 15 minutes with cytochalasin D were subsequently washed with ASW and raised for 15 minutes prior to fixation and immunostaining. Also in 2 cell stage embryos, aPKC activity is required for Par6 (d), but not G_{M1} (e) cortical localization. Embryos were first treated with 10 μ M PKC-zeta peptide inhibitor for 15 minutes then fixed and immunostained for Par6. For G_{M1} localization, embryos were stained with alexa 488 CTB for 30 minutes prior to the inhibitor treatment. Anti-PKC-zeta antibody was used for immunoprecipitation (IP) of 2 cell stage sea urchin embryo lysate. Immunoprecipitates underwent SDS-PAGE and western analysis with anti-PAR6 antibody. Bar equals 50 μ m.

Figure 6

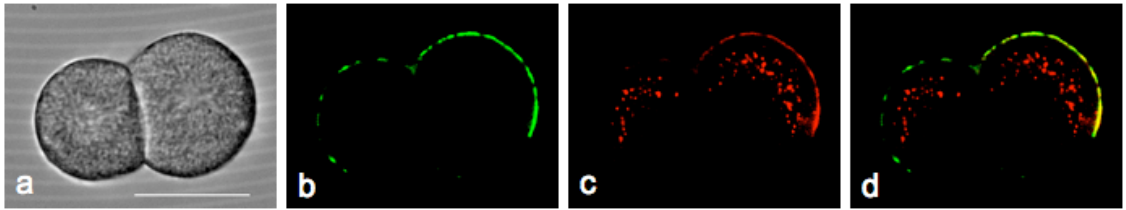


Figure 6: Endocytosis is polarized to the G_{M1} rich apical cell surface. Vesicles (c) are specifically endocytosed at the apical cell surface where G_{M1} localizes (b, d). Embryos were first stained with alexa 488 CTB then dissociated at the 8 cell stage in calcium free seawater prior to incubation with rhodamine labeled dextran for 10 minutes. Excess rhodamine dextran was washed out with calcium free seawater and blastomeres were imaged by spinning disk confocal microscopy. Two blastomeres of an 8 cell stage embryo are shown. Bar equals 25 μm .

Figure 7

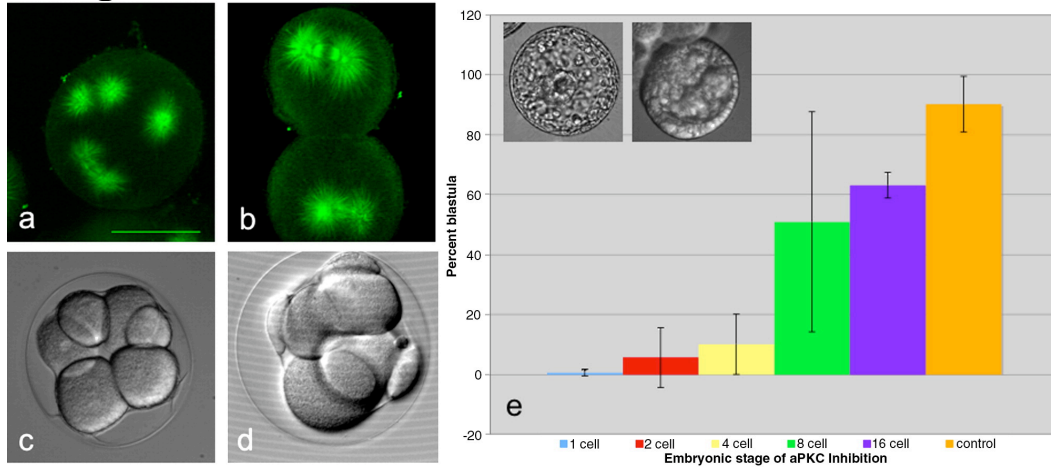


Figure 7: Functional aPKC is required for normal cleavage plane determination and blastula formation. Phenotypes seen after aPKC inhibition included subsequent division of blastomeres into the same plane (c) and birth of unequal sized cells (d). Mitotic apparatus microtubules exhibited many defects including multipolar spindles (a), short asters (b), and improper spindle rotation. 2 cell stage embryos were first treated with 5 μ M PKC-zeta peptide inhibitor and raised through the next cell division before fixation and immunostaining for tubulin. Bar equals 50 μ m. Blastula development was compromised in embryos treated with 4 μ M PKC-zeta peptide inhibitor compared to control (e). The success rate of blastula formation increased as the embryos were treated at later cleavage stages.

Chapter 3: Spatiotemporal Control of the Asymmetrical Membrane Cortex in Cleavage Stage Sea Urchin Embryos

Introduction

The membrane cortex in polarized cells consists of a nonuniform distribution of membrane domains, scaffolding proteins, and polarity determinants. The establishment and maintenance of these components have been a focus for researchers as proper positioning is required for cell migration, cell division, and cellularization, for example. Frequently, cortical domains are polarized within the cell and a variety of molecular mechanisms are responsible for their spatiotemporal control. In migrating cells, which exhibit front-rear polarity, membrane raft microdomains and their associated molecules are preferentially located at the leading membrane cortex. Upon stimulation, the membrane domain patches cluster to the leading edge and their mobility is dependent upon the actin cytoskeleton and cholesterol levels (Manes et al., 1999; Gomex-Mouton et al., 2001). The actin cytoskeleton has also been implicated in membrane domain control in epithelial cells (Oliferenko et al., 1999), the *Drosophila* embryonic syncytium (Mavrakis et al., 2008), T cell activation (Harder and Simons, 1999; Harder and Kuhn, 2000; Bunnell et al., 2002; Wulfing et al., 2000), and mating projection in yeast (Bagnat and Simons, 2002).

Similar to the front-rear polarity of migrating cells, epithelial cells exhibit apical-basolateral polarity, which is bisected by tight junctions. These physical barriers aid in polarity maintenance and are unique to epithelial cells. Membrane microdomains cluster to the apical end of the cell by targeted delivery or selective retention (Yeaman et al.,

1999; Matter, 2000; Schuck and Simons, 2004). The actin cytoskeleton assembles at tight junctions to scaffold signaling networks and reinforce polarity (Clark and Brugge, 1995; Drubin and Nelson, 1996). Although migrating cells and early embryonic cells of *C. elegans* and echinoderms do not have junctions, membrane domains are segregated within the cell and the actin cytoskeleton is partly responsible for this maintenance (Cowan and Hyman, 2007).

Vertebrate neurons also exhibit polarity of membrane domains at the postsynaptic membrane (Sheng and Hoogenraad, 2007; Triller and Choquet, 2005, 2008). Glycophosphatidylinositol (GPI)-anchored proteins, ganglioside G_{M1} , and F actin are concentrated at postsynaptic membranes, giving them membrane raft properties (Renner et al., 2009). These cortical domains are regulated by the actin cytoskeleton and cholesterol levels in the membrane, as in other cell types. Lenne et al. (2006) used fluorescence correlation spectroscopy (FCS) to demonstrate the dependency of membrane domain lateral organization on both lipid composition and the actin cytoskeleton in mammalian culture cells.

In addition to actin, microtubules have also been implicated in the maintenance of membrane cortex asymmetry (Fischer et al., 2008). In *S. pombe* and *A. nidulans*, microtubules interact with the cortex signaling cell-end marker proteins to direct polarized growth (Mata and Nurse, 1997; Sampson and Heath, 2005; Chang, 2006). In addition, Takeshita et al. (2008) noted sterol-rich domains at the growing tips of *A. nidulans*, similar to the polarity seen in migrating cells and in epithelial cells. In epithelial cells, microtubules reinforce apical-basolateral polarity established by tight junctions by asymmetrically orienting in the cell and directing membrane trafficking

(Drubin and Nelson, 1996). Similarly, microtubules initiate cell polarity during wound healing in fibroblasts by stably orienting towards the wound (Gundersen et al., 1998). There, tubulin is post-translationally modified, can recruit intermediate filaments, and interacts with kinesin motor proteins (Gurland and Gundersen, 1995; Liao and Gundersen, 1998). The leading edge is also involved in the integrin-focal adhesion kinase (FAK) signaling pathway through specifically localized G_{MI} -containing membrane domains (Palazzo et al., 2004). In mitotic sea urchin embryos, an equatorial band of ganglioside G_{MI} , glycoproteins, and cholesterol accumulates at mid-anaphase and the movement of these membrane domains is dependent upon microtubules (Ng et al., 2005). This membrane domain asymmetry is also correlated with anaphase onset, myosin light chain phosphorylation, and actin.

Similarly, myosin II (spaghetti squash, sqh) relocates to the furrow region at anaphase in *Drosophila* neuroblasts creating membrane cortex asymmetry (Barros et al., 2003). During prophase and metaphase however, the polarity determinant Lethal giant larvae (Lgl) restricts sqh to the apical cell cortex where it is involved in spatial regulation of polarity (Kalmes et al., 1996). This type of cell cycle dependent movement of the membrane cortex has also been demonstrated by Wirtz-Peitz et al. (2008). The basally localized polarity protein Numb segregates when the mitotic kinase Aurora-A activates the Par polarity complex at the apical cortex, linking Numb localization to the onset of mitosis (Wirtz-Peitz et al, 2008).

Actin and microtubules are cytoskeletal components commonly implicated in polarity regulation; increasingly, however, work has been emerging that demonstrates a role for nonmuscle myosin II in polarity control with respect to cell, planar cell, and

embryonic polarity. For example, nonmuscle myosin II inactivation in *Drosophila* epithelial cells and neuroblasts leads to abnormalities in cell polarity and mitosis (Barros et al., 2003.). Phillips et al. (2005) have demonstrated a role for myosin in planar cell polarity during vertebrate cardiac development. Myocardial cells transition to a polarized migrating cell during this type of development and Rho kinase, a catalyst for myosin phosphorylation and activation, is required. Without myosin phosphorylation, front-rear polarity is disrupted and myocardial cells are not able to invade the cardiac mesenchyme cushion. Eddy et al. (2000) also implicated a role for myosin activation in neutrophil migration. In the absence of myosin light chain kinase (MLCK), another catalyst for myosin phosphorylation, cell polarity is disrupted and inactive myosin is unable to retract the rear of the migrating cell. Asymmetrical localization within the cell of myosin II activators has also been shown (Kolega, 2003). MLCK is active in the cell periphery where it controls membrane ruffling while Rho kinase is at the cell center regulating focal adhesion formation (Totsukawa et al., 2004).

About a decade before Cowan and Hyman (2007) detailed the asymmetric rearrangement of the acto-myosin cytoskeleton after fertilization in *C. elegans* embryos, Guo and Kemphues (1996) demonstrated a requirement for nonmuscle myosin II (NMY-2) in embryonic polarity. Guo and Kemphues found that the posterior localized polarity determinant PAR-1 directly binds to NMY-2 and, using antisense RNA to deplete NMY-2, that NMY-2 is required for proper localization of PAR-1, PAR-2 (posterior), and PAR-3 (anterior). Cowan and Hyman's work was pivotal in providing a molecular mechanism for embryonic polarity establishment and maintenance in *C. elegans*. It is the RhoGAP, CYK-4, and centrosomes contributed by the sperm to the embryo posterior upon

fertilization that initiates asymmetric contractility of the acto-myosin cytoskeleton. The PAR proteins are then physically connected to the acto-myosin network by CDC-42, which is localized to the anterior of the embryo (Aceto et al., 2006; Schonegg and Hyman, 2006).

Although the first cleavage of the sea urchin zygote is symmetric with respect to daughter cell size, the membrane cortex becomes polarized after the first division (Alford et al., 2009). Cytokinesis establishes apical-basolateral cell polarity in sea urchin blastomeres in spite of the absence of cell junctions at this early cleavage stage; ganglioside G_{M1} , a marker for membrane rafts, becomes polarized to the free, or apical, cell surface and remains polarized upon dissociation of the blastomeres. In addition, the PAR complex of polarity proteins becomes apically polarized at the first cell division. However, in contrast to G_{M1} , PAR6 redistributes around the entire cell cortex upon dissociation by Ca^{++} chelation. Blastomeres of early sea urchin embryos are polarized in a manner similar to that of epithelial cells, except for the absence of physical junctions segregating domains.

We became interested in the spatial and temporal controls of this asymmetry as it differs among membrane cortex components in early cleaving echinoderm eggs. Using Fluorescence Recovery After Photobleaching (FRAP) analysis, we found G_{M1} to be mobile only during a narrow window of time beginning at mid-anaphase of the cell cycle and continuing through nuclear envelope formation in the daughter cells. This mobility is largely dependent upon myosin filament assembly but is independent of actin and microtubule depolymerization. Immunofluorescence assays indicated a change in myosin

architecture upon dissociation of blastomeres, thus the dependence of other cortical membrane components on myosin bipolar filaments was also examined.

Lateral organization and regulation of cortical membrane domains and polarity determinants varies among cell types. Thus, we sought to unveil this mechanism in cleavage stage sea urchin embryos. Here, we uncover new evidence demonstrating cell polarity in sea urchin embryos, which emerges at first cleavage. The spatial and temporal polarity control with respect to membrane domains and polarity determinants is also described.

Results

Ganglioside G_{M1} Becomes Mobile in the Membrane Cortex at Mid-Anaphase.

Using fluorescence recovery after photobleaching (FRAP), we first investigated the mobility of the membrane cortex with respect to the cell cycle. We labeled ganglioside G_{M1} with Alexa 488 conjugated cholera toxin subunit B (CTB) and found that this component of the membrane cortex is not mobile until mid-anaphase. Rectangular regions (3x5 μ m) were bleached at either the cell pole or equator of 1, 2, and 4 cell stage embryos before or during nuclear envelope breakdown (NEB) (Fig. 1-2A, Postbleach). G_{M1} did not recover to the bleached region of interest (ROI) during NEB (Fig. 1-2A, 7') or while the cell was in metaphase (Fig. 1-2B, 10') (n=5), whether the ROI was positioned at the cell pole or equator. However, after the chromosomes began to segregate, G_{M1} became mobile and recovered into the bleached region (Fig. 1-2C, 30'') (n=4). Prior to anaphase, the average recovery of fluorescence was 18.1% (SD=11.7) whereas the average recovery after anaphase onset was 73.3% (SD=32.9) (Fig. 2-2A, B). We therefore designated a fluorescence intensity increase greater than 40% within 15 minutes postbleach as recovery in reporting our results (Fig. 2-2B).

To confirm the link between G_{M1} movement and the cell cycle, we arrested CTB-488 labeled cells in metaphase with MG-132, a proteasome inhibitor, and analyzed FRAP of G_{M1}. Rectangular regions (10x20 μ m) bleached at the cell pole or equator failed to show recovery of G_{M1} within 30 minutes (n=5), at which point many cells began to apoptose (data not shown). Cells remained in metaphase and failed to enter into anaphase, demonstrating the lack of G_{M1} mobility during metaphase of the cell cycle. In a

complimentary experiment, urethane treatment, which induces MT catastrophe without affecting mitosis (Strickland et al., 2005), allowed us to observe G_{M1} dynamics specifically during anaphase but in the absence of astral MT-cell cortex interaction. Embryos treated with urethane did show recovery of G_{M1} to bleached ROIs (10x20 μ m) during anaphase (Fig. 1-2D, 6') (n=3) indicating that MT contact to the membrane cortex is not required for increased mobility. Embryos labeled for G_{M1} were bleached at the cell equator or pole 40 minutes after fertilization and ROIs remained bleached in all cells with no recovery of fluorescence until mid-anaphase. This result suggests that membrane mobility was dependent on the anaphase cytoplasm but independent of MT contact with the membrane cortex.

This correlation between anaphase and cortical membrane domain movement was also seen in dissociated blastomeres of 2 and 4 cell stage embryos. G_{M1} in dissociated blastomeres is polarized to the apical cell surface, as previously described (Alford et al., 2009, Fig. 3A), and the plane of the next cell division bisects this crescent-shaped localization pattern. Immediately prior to furrow ingression, G_{M1} rapidly migrates towards the basolateral cell surface and into the cleavage furrow (Fig. 3-2A), presumably to deliver molecules required for cytokinesis (Ng et al., 2005). Interestingly, as the cell divides, G_{M1} clears from the basolateral cell surface, becomes more uniform, and returns to its original localization along the apical membrane (Fig. 3-2A, 15'). In addition, new membrane added to the site of division is free of G_{M1} . To confirm this, CTB conjugated to Alexa 555 was added to cells pre-labeled with CTB-488 30 minutes after the initial furrow ingressed (Fig. 3-2A, 30') and imaged within 5 minutes. CTB-555 colocalized with CTB-488 to the apical cell surfaces and illustrated the lack of G_{M1} on either the

existing or the new basolateral cell surfaces. (Fig. 3-2B). This result illustrates both G_{M1} mobility at mid-anaphase toward the furrow region and its movement back to the apical cell surface at the completion of cytokinesis.

As a positive control for lateral diffusion within the membrane of cleavage stage sea urchin embryos, the dialkylcarbocyanine membrane dye DiO ($DiOC_{18}(3)$) was used for FRAP analysis. Lipophilic carbocyanines are ideal for applications such as FRAP in tracking plasma membrane lipid diffusion because of their affinity for the plasma membrane and small size allowing for free diffusion. DiO moves without restraint within the membrane of 1 and 2 cell stage embryos and recovers to the bleached ROI (data not shown). This result indicates some specific spatiotemporal regulation of G_{M1} mobility in the membrane cortex.

Myosin Filaments Provide Scaffolding for G_{M1} in the Membrane Cortex.

We next investigated possible components of the cytoskeleton that may be responsible for the spatial regulation and control of membrane cortex movement. Formation of the cytokinetic equatorial band of G_{M1} , glycoproteins, and cholesterol requires anaphase onset, actin, microtubules, and myosin filaments (Ng et al., 2005). Wadsworth and colleagues demonstrated the requirement of myosin light chain kinase activity for assembly of the actomyosin contractile ring (2005). Based on this, we used cytoskeletal inhibitors and observed their effect on G_{M1} mobility. Depolymerization of actin by cytochalasin D (CD) or latrunculin B had a minimal effect on the mobility of G_{M1} in the membrane cortex (Fig. 4-2, CD). Embryos were treated with cytochalasin D (10 μ g/ml) at the 1, 2 or 4 cell stage prior to NEB and bleached at equatorial or polar

3x5 μ m rectangular regions. CTB-488 recovery to the bleached ROI was seen prior to anaphase in 25% of the cells (n=8), compared to 0% of control cells (n=5). CD treated cells did not furrow and subsequently became binucleate, indicating the depolymerization of actin but no effect on mitosis. Similar results were seen with latrunculin B (0.2 μ M): 22.2% of treated cells demonstrated recovery of G_{M1} before anaphase (data not shown) (n=9).

To depolymerize microtubules, embryos were treated with nocodazole (Nz) at NEB prior to photobleaching. Treated cells did not proceed through anaphase of mitosis as the spindle was disrupted. Rectangular regions (3x5 μ m, 5x10 μ m, or 5x20 μ m) were bleached at the cell pole or equator of Nz treated 1, 2, or 4 cell stage embryos and analyzed for recovery prior to anaphase (Fig. 4-2, Nz). Depolymerization of microtubules did have an effect on G_{M1} maintenance prior to anaphase: recovery to the bleached region was seen in 36.8%, 22.2%, and 43.0% of embryos treated with 1 μ M (n=19), 0.1 μ M (n=9), or 0.01 μ M (n=7) Nz respectively.

In contrast to actin and microtubules, myosin filament assembly plays a significant role in anchoring the membrane cortex prior to anaphase. We used inhibitors of myosin light chain phosphorylation by myosin light chain kinase, ML-7 and ML-9, or the Rho kinase inhibitor, H1152, to prevent myosin filament assembly prior to photobleaching. Rectangular regions of various sizes (3x5 μ m, 5x5 μ m, 5x7.5 μ m, 5x20 μ m, or 10x20 μ m) were bleached in cells prior to NEB after drug treatments and followed for recovery of G_{M1} to the ROI. When treated with ML-7 (100 μ M), G_{M1} moved into the ROI in 80% of 1, 2, and 4 cell embryos (n=10) prior to anaphase, indicating a role for myosin light chain phosphorylation by myosin light chain kinase (MLCK) in

membrane cortex stability (Fig. 4-2, ML-7). Similarly, embryos treated with ML-9 (120 μ M) prior to or at NEB exhibited recovery of G_{M1} to the bleached region in 75% of cells (Fig. 4-2, ML-9) (n=4). When Rho kinase was specifically inhibited with the small molecule H1152, 61.5% of 1, 2, and 4 cell stage embryos (n=13) demonstrated movement of G_{M1} into the bleached region prior to anaphase (Fig. 4-2, H1152). Taken together, these data suggest a role for myosin filament assembly in the regulation of G_{M1} mobility within the membrane cortex (Table 1).

Interestingly, we found the effect of myosin light chain phosphorylation inhibition on G_{M1} mobility to be enhanced in blastomeres dissociated by chelating calcium. As we previously reported, ML-7, in contrast to nocodazole, cytochalasin D, and blebbistatin, caused apical G_{M1} localization to redistribute around the entire cortex in dissociated blastomeres (Alford et al., 2009). In an extension to this finding, we bleached G_{M1} labeled with CTB-488 in dissociated blastomeres treated with ML-7 (100 μ M), ML-9 (120 μ M), or H1152 (2.5 μ g/ml) and analyzed the ROI for recovery before anaphase onset. In a control experiment, 25% of untreated dissociated blastomeres showed recovery to the bleached ROI prior to anaphase (n=4) (Table 2). In contrast, dissociated blastomeres of 2 and 4 cell stage embryos showed recovery of G_{M1} to the bleached region in 100% of those treated with ML-7 (n=5) or H1152 (n=5) (Fig. 5-2). In 80% of those exhibiting movement of G_{M1}, recovery to the ROI (5x10 μ m) occurred within 6 minutes of bleaching. When dissociated blastomeres were treated with ML-9 prior to NEB and bleaching, recovery to the bleached region was seen in 83.3% of the cells (n=6) and occurred between 3.5 and 14 minutes (Fig. 5-2, ML-9). Thus, calcium-dependent

adhesion between blastomeres appears to play a role in the regulation of G_{M1} mobility along with myosin filament assembly (Table 2).

Myosin Distribution Changes in Dissociated Blastomeres

Interestingly, G_{M1} mobility is increased within the membrane of 2 and 4 cell stage blastomeres dissociated by chelating Ca^{++} when treated to inhibit myosin filament assembly. The average percent of 1, 2, and 4 cell stage embryos treated with ML-7, ML-9, or H1152 in which G_{M1} recovered to the bleached ROI was 72.1%, whereas recovery in those that had been dissociated and drug treated was 94.4% (Table 2).

To determine if myosin distribution changes upon dissociation of early embryos, we immunostained intact and dissociated early embryos for total myosin and compared their localization patterns. Although myosin is globally present within the cell, 2 and 4 cell stage embryos exhibit increased myosin localization to the apical, or free, cell cortex relative to the basolateral cell cortex. Mean fluorescence intensity at the apical cortex is 102.5 and 128.2 in 2 and 4 cell stage embryos, respectively (Fig. 6-2A, B). This is a 5.3 average fold increase in intensity compared to the basolateral cortex, which is 28.7 and 18 in 2 and 4 cell stage embryos, respectively (Fig. 6-2B). The difference in apical versus basolateral cell surface fluorescence intensity is significant with respect to the standard deviation and t-test ($p=0.001$, 2 cell stage, $n=5$; $p=6.6E^{-9}$, 4 cell stage, $n=7$) (Fig. 6-2B). In contrast, the fluorescence intensity of total myosin of the apical cell surface compared to that of the basolateral cell surface in dissociated blastomeres of 2 and 4 cell stage embryos is not statistically different ($n=25$). The average intensity of the apical cortex is 123.3 ± 27 in dissociated blastomeres whereas that for the basolateral cortex is

92.5±38.1 (Fig. 6-2A, B). With respect to a t-test, the average fluorescence intensity of the basolateral cell surface is not statistically different than that of the apical cell surface ($p=0.001$). Immunofluorescence of phosphorylated myosin in intact 2 and 4 cell stage embryos did not show specific localization to the apical cortex. Rather, our results confirmed those of Mabuchi (2008) and Shuster (2006). Phosphomyosin localization was concentrated at the furrow region in dividing embryos (Fig. 6-2C). In dissociated blastomeres non-dividing, phosphomyosin was nonspecifically localized and minimal signal was detected in the cell (data not shown). Isolation of detergent resistant membranes revealed the presence of myosin in raft fractions as well as in cytoplasmic and particulate lysate fractions (Fig. 6-2D). This indicates the association of myosin with membrane domains supporting a role for myosin scaffolding of G_{M1} .

In dissociated blastomeres, total myosin is less distinctly localized to the apical cortex, possibly accounting for the difference in G_{M1} mobility in associated embryos versus dissociated blastomeres. This change in myosin distribution may also explain the change in PAR6 localization upon dissociation. The polarity determinant PAR6 is localized to the apical cell cortex in intact 2 and 4 cell stage embryos, but, similar to myosin, redistributes around the entire cell cortex upon dissociation. (Alford et al., 2009)

Myosin Light Chain Kinase Provides Scaffolding for Polarity Proteins Par6, aPKC, and Cdc42.

Previously, we noted the establishment of polarity proteins Par6, aPKC, and Cdc42 to the apical cell surface after the first cleavage division in sea urchin embryos. Since Par6 and Cdc42 redistribute around the entire cortex in dissociated blastomeres of

2 and 4 cell stage embryos similar to total myosin, we looked at the effects of myosin filament assembly inhibition on their localization in associated early embryos. Treatment of intact 2 cell stage embryos (prior to NEB) with ML-7 (100 μ M) 15 minutes prior to fixation caused Par6, aPKC, and Cdc42 to lose their cortical localization (Fig. 7-2, ML-7). This diffuse localization with respect to the cortex was also seen in embryos treated with ML-9 (120 μ M) 15 minutes prior to fixation (Fig. 7-2, ML-9).

Inhibition of Rho kinase with H1152, in contrast, did not affect the apical localization of Par6, aPKC, or Cdc42 (Fig. 7-2, H1152). Since both ML-7 and ML-9 inhibit the activity of myosin light chain kinase (MLCK) whereas H1152 inhibits that of Rho kinase, MLCK and not Rho kinase appears to play a role in the maintenance of Par6, aPKC, and Cdc42 apical localization.

Discussion

In the present study, we identified nonmuscle myosin II as the major spatial regulator of asymmetry in early sea urchin embryos. Myosin filaments provide scaffolding for ganglioside G_{M1} in the membrane cortex as well as the polarity determinants Par6, aPKC, and Cdc42. Apical-basolateral polarity of membrane and cortical domains is established by cytokinesis at first cleavage in sea urchin embryos (Alford et al., 2009). The polarity in sea urchin embryos resembles that of epithelial cells where membrane domains rich in cholesterol and G_{M1} are localized to the apical cell surface as well as the PAR complex consisting of Par6, Par3, and aPKC. Interestingly, we find that myosin localization in blastomeres changes upon dissociation from intact 2 and 4 cell stage embryos. This difference may account for both the increased mobility of

the membrane cortex and the redistribution of polarity determinants upon dissociation by Ca^{2+} chelation.

Previously, we found G_{M1} to be evenly distributed around the sea urchin zygote membrane, form an equatorial band at mid-anaphase, and become polarized to the apical cell surface at first cleavage (Ng et al., 2005; Alford et al., 2009). We began our investigation of sea urchin embryo membrane asymmetry by asking when G_{M1} is mobile within the membrane. Fluorescence recovery after photobleaching (FRAP) analysis indicates that G_{M1} mobility is not correlated with its polarization to the apical membrane cortex at the first cleavage. Rather, we observed correlation of G_{M1} mobility with the cell cycle, specifically mid-anaphase. G_{M1} free lateral diffusion corresponds with the formation of the equatorial band of actin, myosin, and cholesterol during cytokinesis.

To uncover the spatial molecular controls of this anaphase-coordinated mobility, we disrupted various cytoskeletal components prior to photobleaching. Although actin and microtubule depolymerization somewhat affect G_{M1} mobility, myosin bipolar filament assembly significantly anchor G_{M1} in the membrane. When intact embryos were treated with cytochalasin D, Latrunculin B, or nocodazole, fluorescence recovery to the bleached region was seen in 25%, 22.2%, or 34% of the cells, respectively. Myosin inactivation caused G_{M1} mobility in 72.1% of embryos before anaphase. These results are consistent with a finding from our previous study of G_{M1} polarity. MLCK inhibition causes G_{M1} redistribution around the entire cell membrane in dissociated blastomeres whereas actin or microtubule depolymerization alone does not (Alford et al., 2009). Thus, we provide new evidence for a role of active myosin in G_{M1} spatial regulation.

An additional factor that contributes to the anchoring of G_{M1} is calcium dependent cell adhesion. This factor surfaced when we dissociated blastomeres and then treated with myosin phosphorylation inhibitors. The free lateral diffusion observed in ML-7, ML-9 and H1152 treated intact embryos was augmented in dissociated, treated embryos. The results from FRAP analysis clearly demonstrate this: 72.1% of intact 2 and 4 cell stage embryos and 94.4% of dissociated blastomeres demonstrated G_{M1} recovery to the bleached region prior to anaphase. This is most interesting as junctions have yet to form between blastomeres of 2 and 4 cell stage embryos, which act as physical barriers controlling apical-basolateral polarity in epithelial cells. Therefore, the physical contact between sea urchin blastomeres aids in the restriction of membrane domains to the apical cell surface.

After a closer look at myosin architecture in intact and dissociated embryos, myosin appears to be concentrated at the apical cortex. Immunofluorescence analysis of total myosin illustrates an intensity at the apical cortex of 115.4 versus 23.4 at the basolateral cortex in associated embryos. The polarity of myosin concentration to the apical surface is lost upon dissociation. A statistical t-test comparing the mean fluorescence intensity at the apical versus basolateral cell cortices in dissociated blastomeres does not render the fluorescence intensities significantly different.

Myosin also plays a role in the asymmetric localization of PAR-3, which has been shown in *C. elegans* (Guo and Kemphues, 1996). Additionally, asymmetrical actomyosin contraction throughout the *C. elegans* embryo is responsible for PAR complex polarity, anchored to the actomyosin network by CDC-42 (Cowan and Hyman, 2007). In cleavage stage sea urchin embryos, PAR6 is found at the apical cell cortex in

addition to Cdc42, a small GTPase involved in polarity establishment and maintenance in a variety of cell types (Alford et al., 2009). In this study, aPKC was also found to be preferentially localized to the apical cell surface. Disruption of myosin filament assembly by ML-7 or ML-9, inhibitors of myosin light chain kinase, caused PAR6, Cdc42, and aPKC to have a more diffuse localization throughout the cytosol. These data suggest a scaffolding role for filamentous myosin in localizing the Par complex. However, inhibition of Rho kinase by H1152, did not affect the cortical localization of these polarity determinants.

In fact, however, myosin's role in polarity is controversial among researchers. Myosin II was thought to restrict specific polarity determinants from the apical cortex through a negatively regulated cascade involving aPKC, Lgl, and Miranda, a neuronal differentiation factor (Barros et al., 2003; Ohshiro et al., 2000; Peng et al., 2000; Betschinger et al., 2003). Mutational and pharmacological studies demonstrated a role for Lgl in regulating myosin activity and apical localization (De Lorenzo et al., 1999; Barros et al., 2003). Atwood and Prehoda (2009) recently questioned a definitive role for myosin II in polarity establishment in *Drosophila* neuroblast division. Removing myosin II from the polarity cascade, they found Miranda to be a direct substrate for aPKC and this phosphorylation event is sufficient to displace Miranda from the apical cortex. Intriguingly, Atwood and Prehoda found that the Rho kinase inhibitor used to implicate myosin II in polarity maintenance was a more effective inhibitor of aPKC activity.

In conclusion, asymmetry of the sea urchin embryo membrane cortex is regulated by the cell cycle and the cytoskeleton, specifically filamentous myosin. The timing of membrane domain mobility is correlated with anaphase, when molecules required for

cytokinesis must be delivered to the furrow region. Spatially, bipolar myosin filaments play the most significant role in membrane cortex control, both with respect to membrane domains and cortically localized polarity determinants.

Figure 1-2

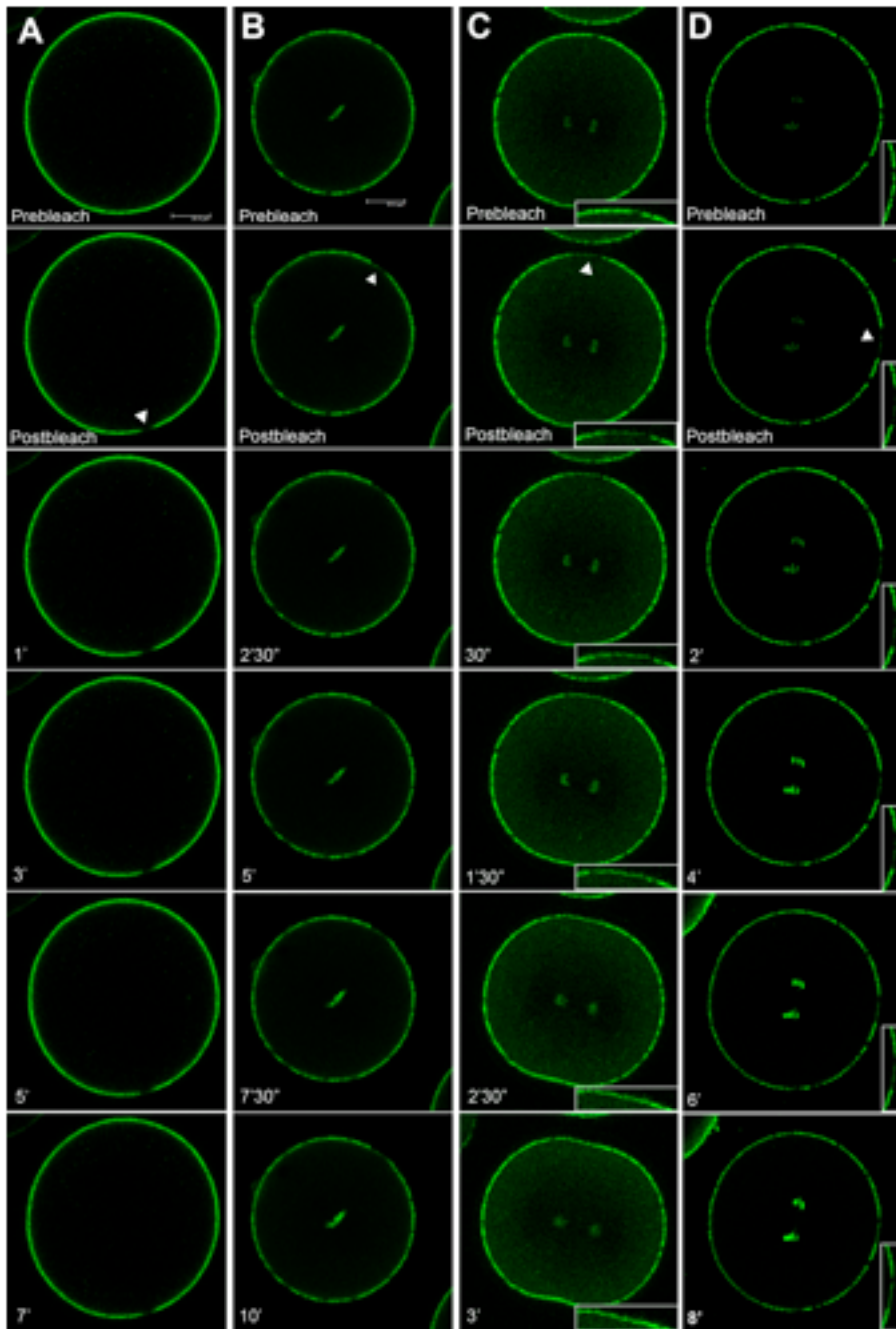
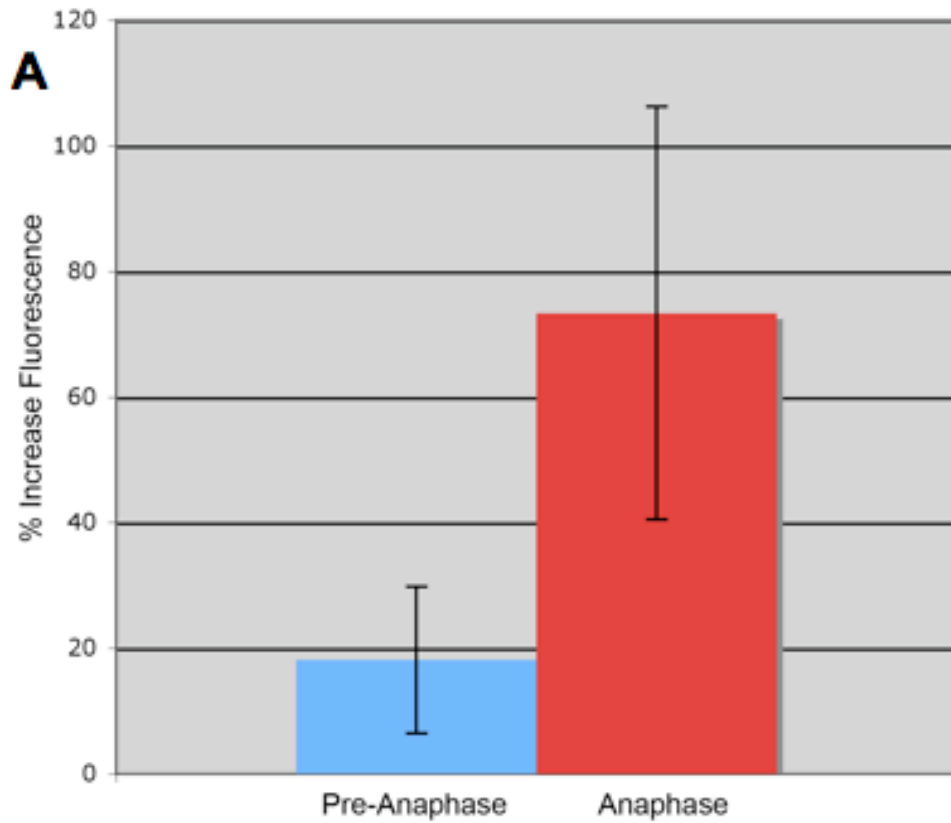


Figure 1: Ganglioside G_{M1} recovers to the bleach region of interest at mid-anaphase.

A) Embryo stained with CTB-488 is bleached at the equator 45 minutes post-fertilization, at NEB. Recovery is not observed to the bleached ROI (3x5 μ m) within 7 minutes, when metaphase begins. B) Embryo stained for G_{M1} bleached at the cell equator 60 minutes post-fertilization shows no recovery during metaphase. ROI remains bleached for 10 minutes, prior to anaphase onset. C) Equatorial ROI was bleached during early anaphase and followed for recovery. At the anaphase A to B transition as the cell begins to elongate, G_{M1} moves into the ROI (inset) within 1 minute postbleach. D) Embryo treated with urethane progresses through anaphase, but does not furrow due to lack of astral microtubules. Recovery of G_{M1} to the equatorial bleached ROI is seen within 2 minutes and demonstrates G_{M1} mobility during anaphase. Chromosomal staining in bleed-through of Hoescht labeling. Scale bar equals 25 μ m.

Figure 2-2



B

	Avg. % Increase Fluorescence	Std. Dev.
Pre-Anaphase	18.1	11.7
Anaphase	73.3	32.9

Recovery > 40%
Lack of Recovery \leq 40%

Figure 2: Fluorescence intensity increase greater than 40% to the bleached ROI is designated as recovery. A) Analysis of untreated embryos reveals a statistically significant difference in fluorescent intensity after photobleaching to the region of interest (ROI) prior to anaphase versus during anaphase. B) Average percent increase in fluorescence intensity prior to anaphase is 18.1% with a standard deviation of 11.7. After anaphase onset, the average percent increase in fluorescence intensity is 73.3% with a standard deviation of 32.9. The range for pre-anaphase embryos is 6.4 – 29.8% and 40.4 – 106.2%. A percent increase in fluorescence to the bleached ROI greater than 40% is thus scored as recovery.

Figure 3-2

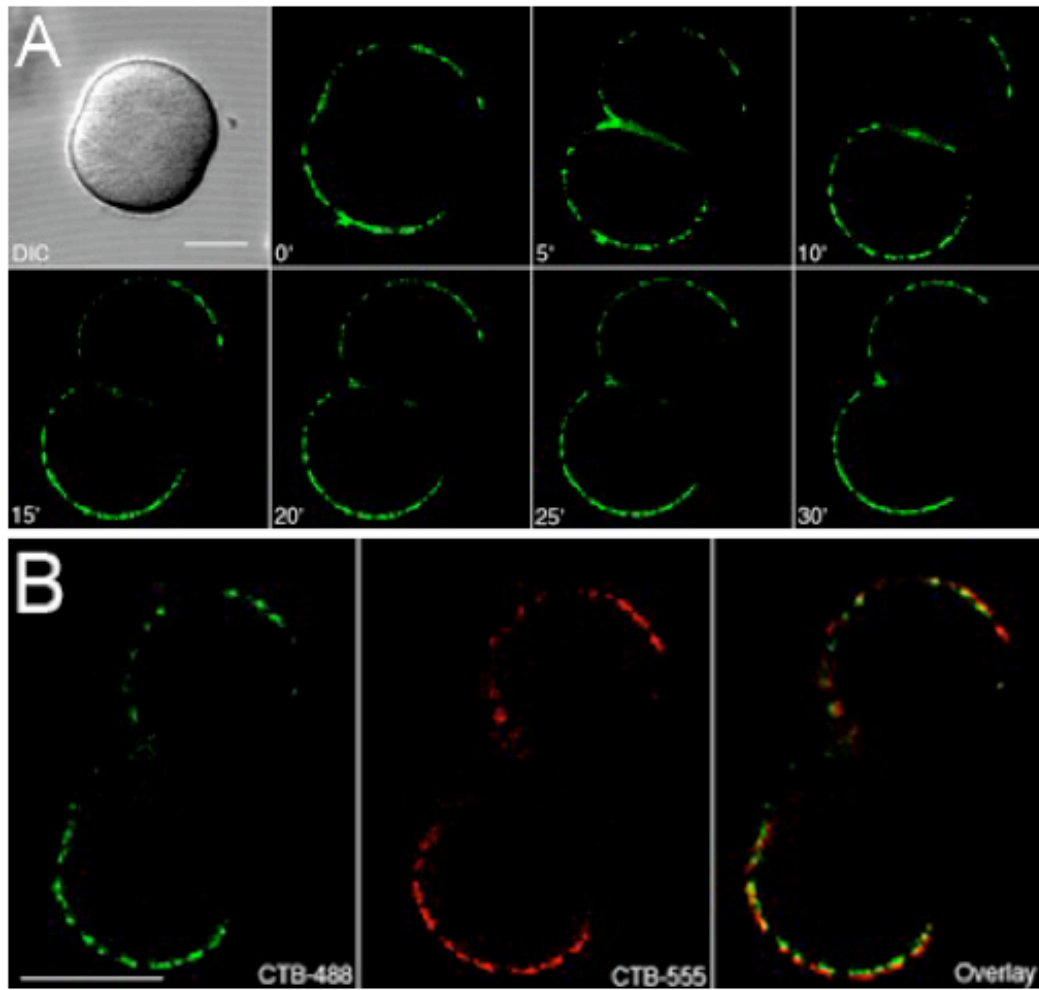


Figure 3: Ganglioside G_{M1} polarized to the apical membrane cortex in dissociated blastomeres migrates into the basolateral furrow and subsequently clears. A) G_{M1} in a dissociated blastomere from a 4 cell stage embryo is polarized to the apical membrane, however, at anaphase, migrates into the cleavage furrow (5'). As new membrane is added during division, G_{M1} clears from the basolateral surface and returns to the apical membrane (20'). B) New membrane is free of G_{M1} indicated by CTB-555 staining solely to the apical membrane cortex. Scale bar equals 25 μ m.

Figure 4-2

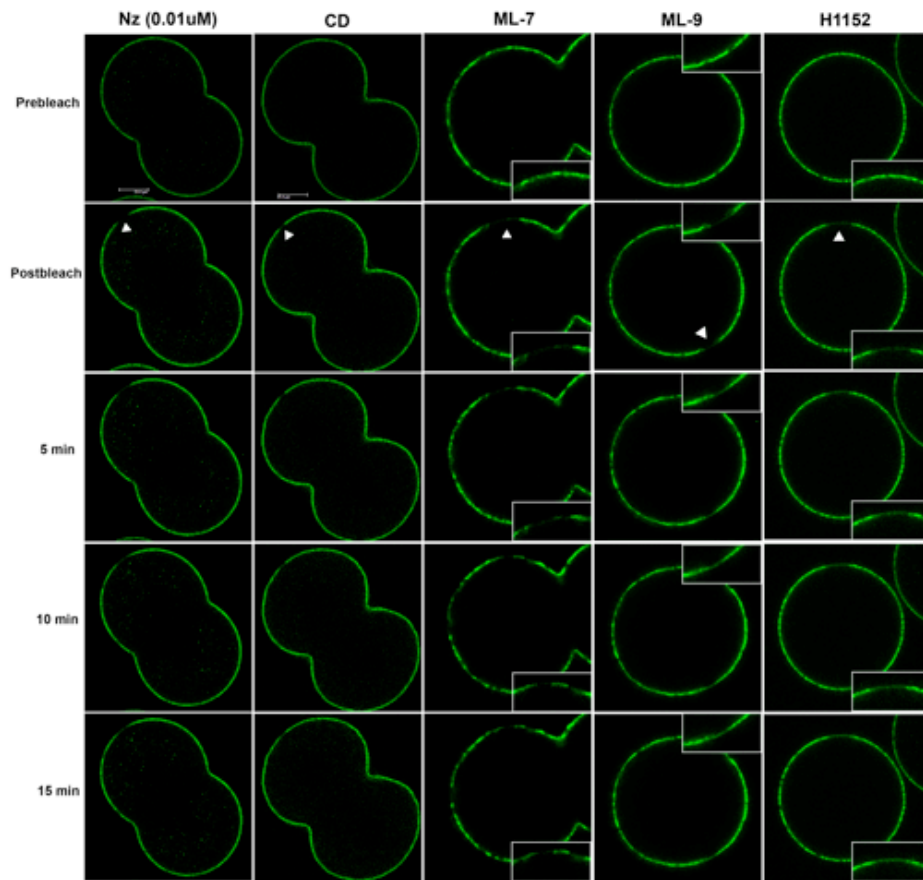


Figure 4: Myosin filaments play a larger role in G_{M1} scaffolding than microtubules or actin. One or two cell stage embryos were bleached at NEB following treatments with 0.01 μ M nocodazole (Nz), 10 μ g/ml cytochalasin D (CD), 100 μ M ML-7, 120 μ M ML-9, or 2.5 μ g/ml H1152 and analyzed for recovery prior to anaphase. Recovery of G_{M1} to the bleached ROI in ML-7, ML-9, and H1152 treated embryos is seen within 5 minutes whereas recovery in Nz and CD treated cells is seen in 42.9% and 25% of embryos, respectively. Scale bar equals 25 μ m.

Figure 5-2

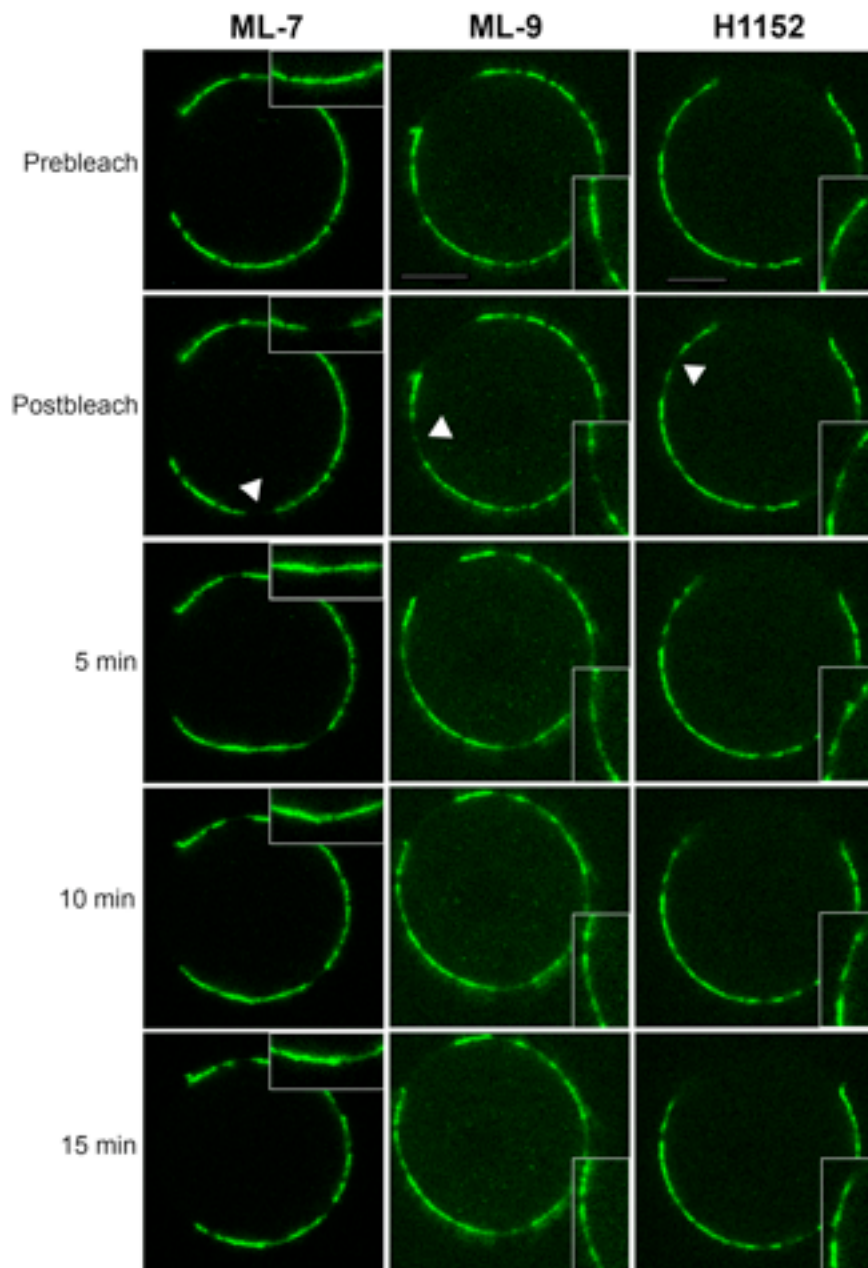


Figure 5: Dissociation of blastomeres increases G_{M1} mobility in the membrane cortex. Dissociated blastomeres of 2 and 4 cell stage embryos show increased mobility of G_{M1} compared to intact embryos when treated with myosin filament assembly inhibitors. 100% of dissociated blastomeres treated with ML-7 or H1152 showed G_{M1} recovery to the ROI. 83.3% of blastomeres treated with ML-9 demonstrated recovery to the ROI. G_{M1} recovery was seen within 5 minutes regardless of the ROI location in the membrane cortex. Scale bar equals 25 μ m.

Figure 6-2A

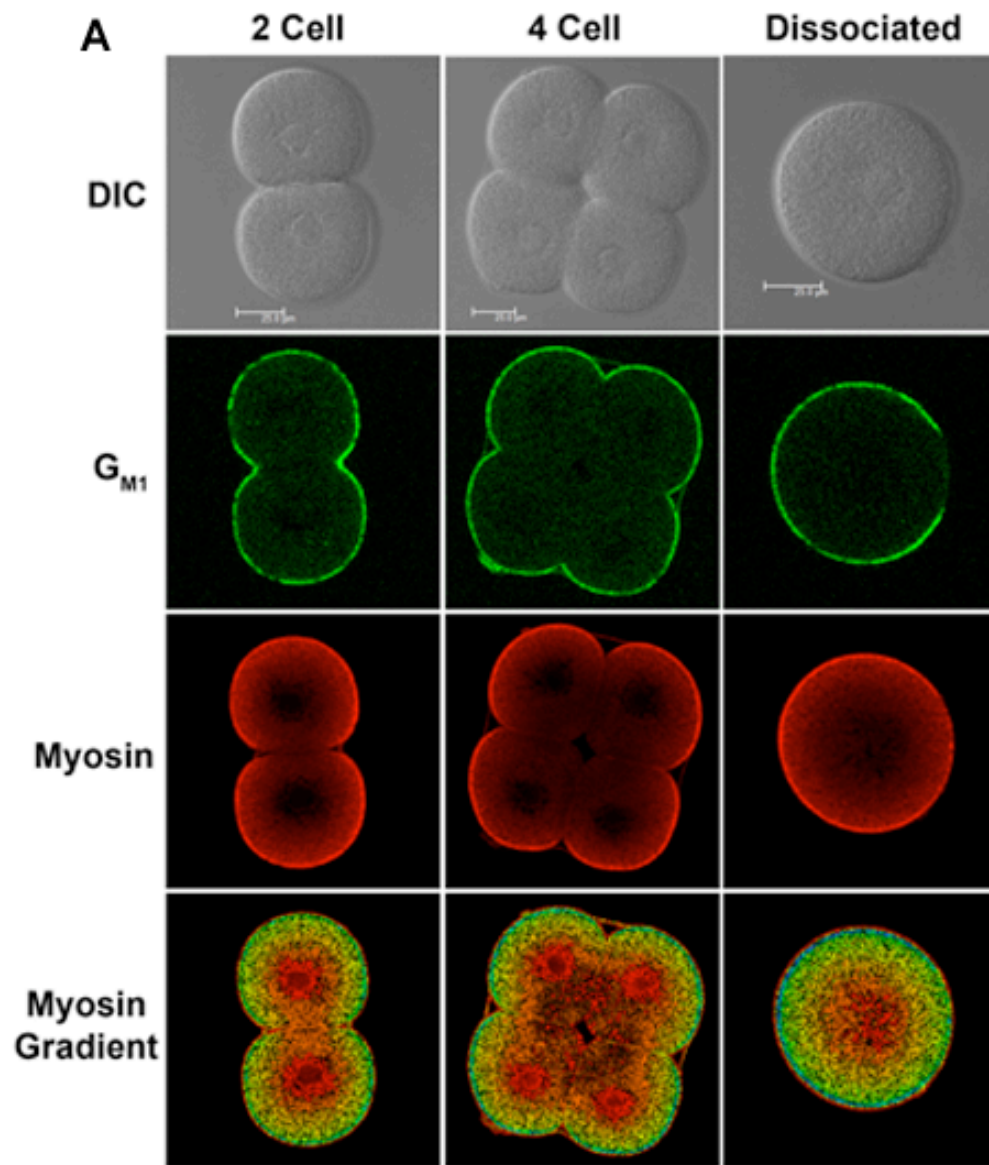


Figure 6-2B

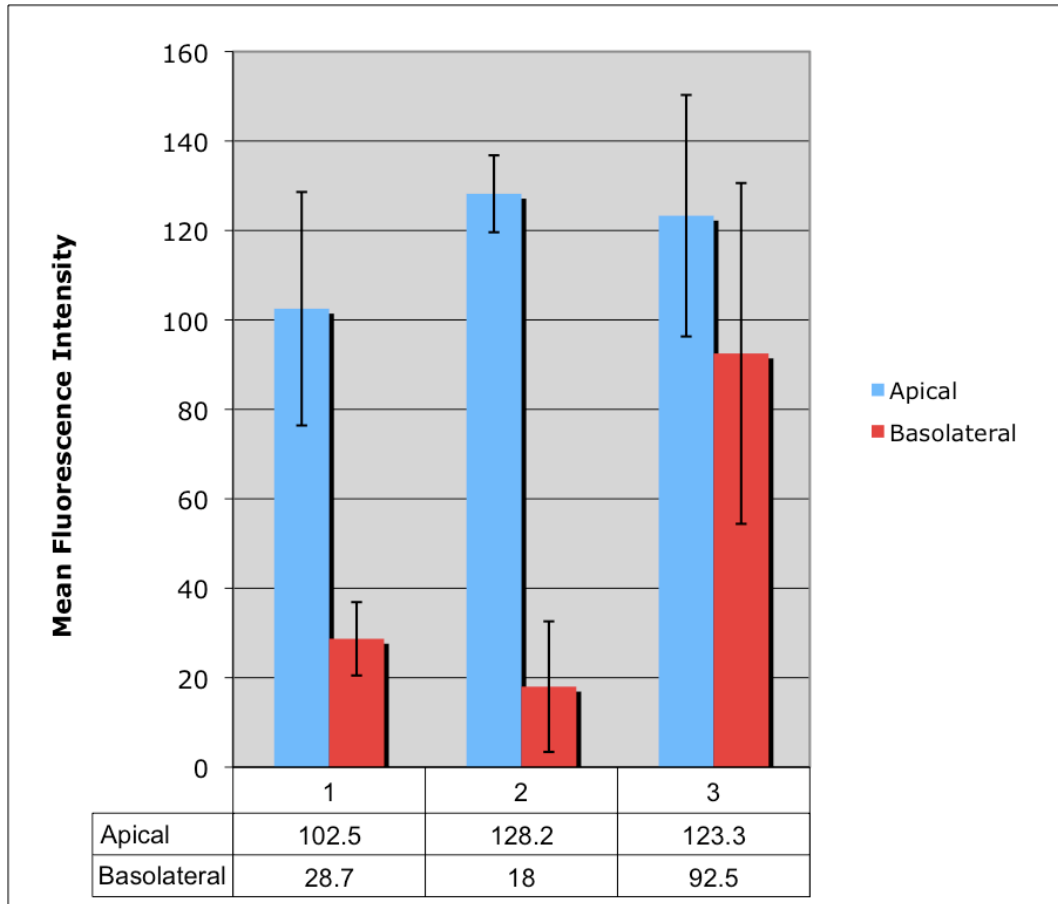


Figure 6-2C

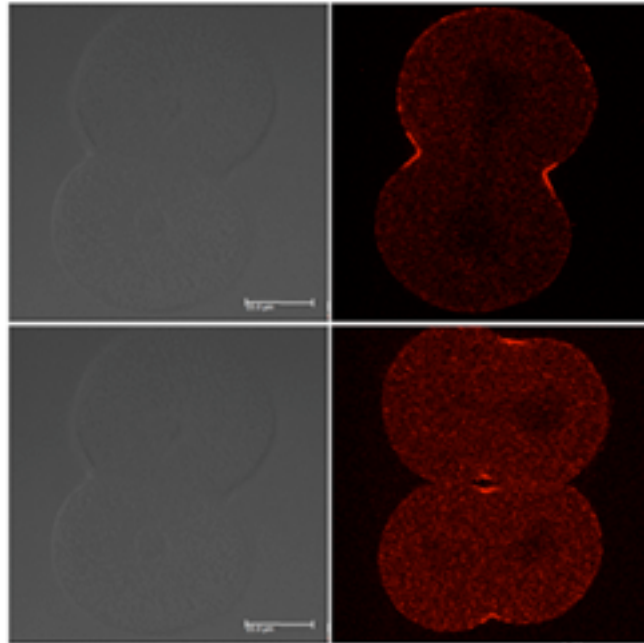


Figure 6-2D



Figure 6: Myosin localization changes upon dissociation of 2 and 4 cell stage embryos. A) G_{M1} staining is used as a marker for the apical membrane cortex. Myosin also localizes to the apical cortex in intact embryos. In dissociated blastomeres, this trend is seen with a gradient pseudocolor, however the difference in fluorescence intensity at the apical versus basolateral cortex is not statistically significant. B) Graphical representation of total myosin mean fluorescent intensity at apical versus basolateral cortex in intact and dissociated embryos. In intact 2 and 4 cell stage embryos, total myosin fluorescence is significantly greater at the apical cortex than that at the basolateral cortex. In contrast, there is no significant difference in myosin fluorescence at the apical and basolateral cortex in dissociated blastomeres. C) Phosphorylated myosin is localized to the furrow region in mitotic sea urchin blastomeres. Scale bar equals $25\mu\text{m}$. D) Immunoblot of isolated detergent resistant membranes reveals presence of total myosin II in the cytoplasmic fraction (cyto), the particulate lysate (lysate), and flotation fractions 3 and 4 of 2 cell stage embryos.

Figure 7-2

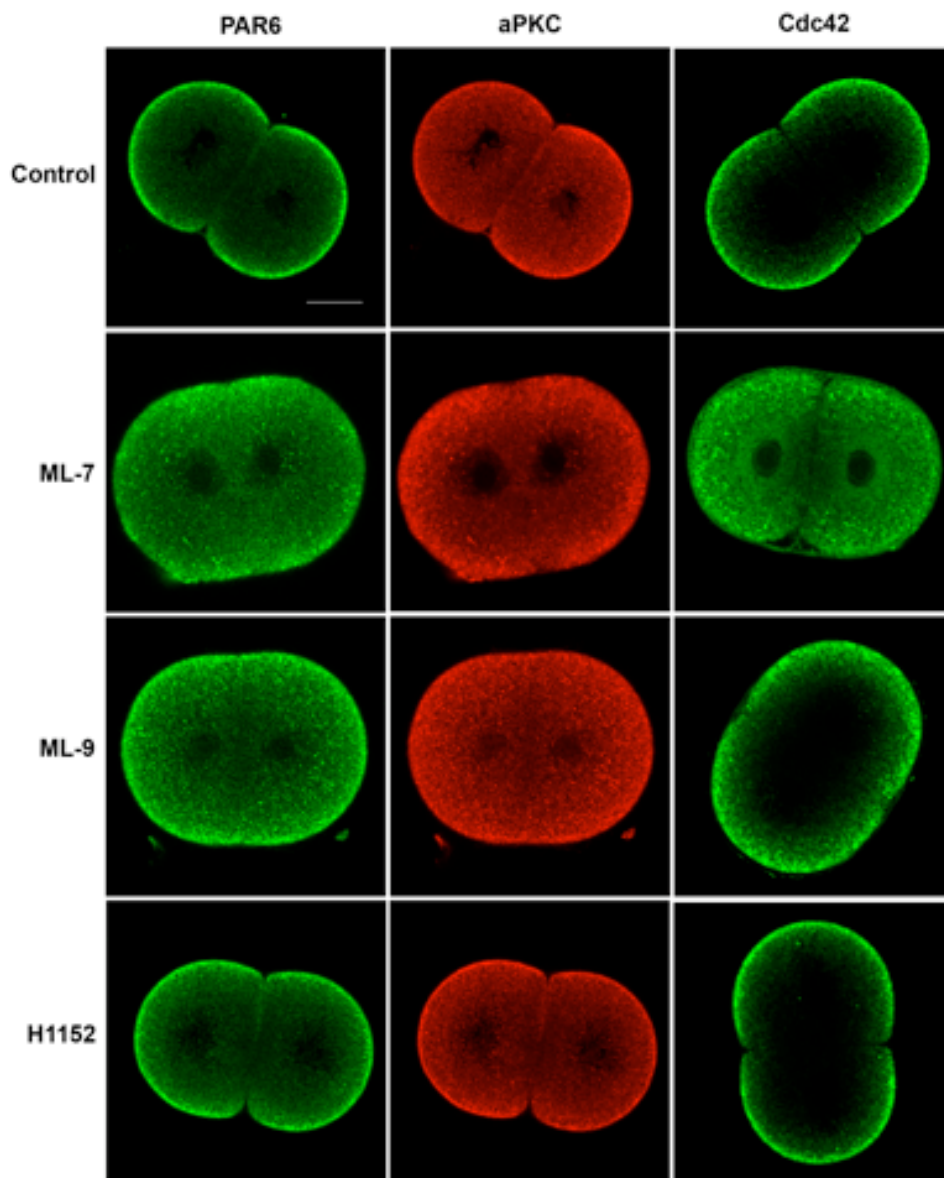


Figure 7: Inhibition of myosin light chain kinase disrupts PAR6, aPKC, and Cdc42 apical localization. Treatment of ML-7 or ML-9 affects the localization pattern of the polarity proteins PAR6, aPKC, and Cdc42 to the apical cortex. In contrast, the Rho kinase inhibitor H1152 does not alter the apical polarization of PAR6, aPKC, and Cdc42. Scale bar equals 25 μ m.

Inhibitor	Dose	n	% Recovered Pre-anaphase
-	-	9	0
Nz	1 μ M	19	36.8
	0.1 μ M	9	22.2
	0.01 μ M	7	42.9
CD	10 μ g/ml	8	25
Latrunculin B	0.2 μ M	9	22.2
ML-7	100 μ M	10	80
ML-9	120 μ M	4	75
H1152	2.5 μ g/ml	13	61.5

Table 1: Inhibition of myosin filament assembly increases G_{M1} mobility more than Nz or CD treatments compared to control. Untreated embryos do not show G_{M1} mobility prior to anaphase whereas treatment with cytoskeletal inhibitors causes G_{M1} movement within the membrane cortex pre-anaphase. Fluorescence intensity increase to the bleached ROI greater than 40% of the loss of fluorescence was scored as recovery (Fig. 1).

Inhibitor	% Intact Embryos	% Dissociated Blastomeres (n)
-	0	25 (4)
ML-7	80	100 (5)
ML-9	75	83.3 (6)
H1152	61.5	100 (6)
Avg. with inhibitors	72.1	94.4

Table 2: Dissociation of blastomeres increases G_{M1} mobility prior to anaphase.

Ganglioside G_{M1} recovers to the bleached region of interest prior to anaphase in 25% of control dissociated blastomeres, compared to 0% of intact control embryos. In addition, dissociation of blastomeres previously treated with MLCK or Rho kinase inhibitors increases G_{M1} mobility compared to intact, treated embryos. Inhibition of myosin filament assembly induced G_{M1} recovery in 72.1% of intact embryos as opposed to 94.4% of dissociated blastomeres.

Chapter 4: Discussion

The lack of work on early deuterostome embryonic polarity lends itself to the need for a model deuterostome. Here, I have investigated polarity established by the first cleavages in sea urchin embryos, a model deuterostome, revealing precocious embryonic polarity. A significant amount of research has contributed to our understanding of polarity establishment and maintenance in the protostome *C. elegans* and *Drosophila*, for example, but that in deuterostomes has focused on later developmental stages, as discussed in this thesis. In the sea urchin embryo, asymmetries in the membrane and cell cortex are set up as early as the first cell division after fertilization. These asymmetries are required for proper spindle alignment and cleavage plane determination and are responsible for polarized fluid phase endocytosis.

The sea urchin zygote plasma membrane and cortex are segregated into distinct domains at the first cell division by new membrane insertion into the cleavage furrow. The new or basolateral membrane, at the cell-cell contact site, remains distinct from the apical, or contact-free, cell surface despite a lack of junctions at this early stage of development. In fact, junctions do not form until cells of the blastula become an epithelium after asymmetrical blastomere divisions commence at the 16 cell stage.

Markers of the apical cell surface, of membrane domains, and of conserved polarity proteins illustrate early deuterostome embryonic polarity in 2 and 4 cell stage embryos. Inoue (1990) had noted the accumulation of pigment granules in the furrow of dividing sea urchin zygotes just after Schroeder (1988) characterized apically localized pigment granules and microvilli in early sea urchin embryos. Burke (2004), using

antisense morpholinos, suggested that the cortical actin cytoskeleton is anchored by betaC integrins in fertilized sea urchin eggs. Ganglioside G_{M1}, a lipid raft marker, accumulates in the cleavage furrow of dividing sea urchin embryos and subsequently clears, localizing to the apical cell surface (Alford et al., 2009). We also found betaC integrins and the polarity determinants Par6, aPKC, and Cdc42 at the apical cell surface in 2 and 4 cell stage embryos (Alford et al., 2009).

My investigation into the spatial regulation of polarity in cleavage stage sea urchin embryos revealed somewhat different controls for membrane domains and cortical polarity determinants. Myosin filaments play a role in the spatial regulation of both membrane domains and the Par complex whereas an intact actin cytoskeleton is required for proper Par localization, not that of membrane domains. Microtubules are not involved in early sea urchin embryo polarity as it is in the cell polarity of yeast (Mata and Nurse, 1997; Sampson and Heath, 2005) or migrating fibroblasts (Gundersen et al., 1998; Gurland and Gundersen, 1995).

How myosin filaments scaffold membrane domains and cortical polarity proteins remains a question, and several possible mechanisms are worth examining. It is interesting to note that membrane domains, represented here by the ganglioside G_{M1}, differ in their behavior upon dissociation of blastomeres from that of the Par complex. Par6, for example, redistributes around the entire cortex of dissociated blastomeres, indicating the presence of restricting molecules at the blastomere-blastomere contact site. Myosin architecture also changes upon dissociation therefore, the same cellular component could be contributing to Par protein and myosin restriction.

In an effort to identify possible restrictors between blastomeres, I examined the localization of known cell-adhesion molecules and scaffolding cytoskeletal binding proteins. Although Miller and McClay (1997) published data indicating the presence of β -catenin and cadherin at cell-cell contacts in 2 and 4 cell stage embryos, I was not able to duplicate this result. β -catenin and cadherin were present between blastomeres, but not any more specifically than at apical regions of the cell cortex. I conclude that neither β -catenin nor cadherin play a significant role in the restriction of the Par complex, myosin or G_{M1} from the contact site between blastomeres. If disruption of these adhesion molecules does not affect polarized distribution of the Par complex, myosin or G_{M1} in intact embryos, then we can confirm this assumption.

In addition, I examined the localization of septin, an actin-binding scaffolding protein. Septin, localized to the neck of a new bud site in dividing yeast cells (McMurray and Thorner, 2009; Weirich, 2008), is localized to the apical cell surface in sea urchin blastomeres. Preliminary results indicate that disruption of septin by forchlorfenuron (Hu et al., 2008) does not disrupt G_{M1} apical distribution. Septin redistribution around the entire cortex upon dissociation needs to be confirmed as well as spectrin. Spectrin, another actin binding protein known to play a role in scaffolding (Thomas, 2001; Chen et al., 2009), is not specifically localized to the apical cortex in 2 and 4 cell stage embryos. Rather, preliminary data showed spectrin distribution around the entire cortex, likely negating a role for it in basolateral exclusion.

An alternative approach to deciphering what is restricting Par6 from the basolateral cell surface in associated 2 and 4 cell stage embryos involves live cell imaging of the Par complex. Par6 has been successfully cloned into an EGFP fusion

vector and upon bacterial expression, remains in exclusion bodies (construct gift from W.J.Nelson, Stanford University). Currently, Cdc42 is being cloned to create a GFP fusion protein as well (construct from Guthrie cDNA Resource Center, Missouri University). With fluorescent fusion proteins, blastomeres of early sea urchin embryos could be dissociated by micromanipulation and the timing of redistribution could be analyzed. Subsequently, blastomeres could be reassociated to look for clearing from the new cell-cell contact site. If Par6 did clear from the new contact site, then the basolateral surface may not be as important in restriction as the physical contact between cells. If clearing does not occur, then likely there exists molecules specifically localized to the basolateral cell surface responsible for restricting the Par complex upon contact.

Also of interest for future directions is the contact-independent polarization of G_{M1} . Reassociation experiments described above have been performed with G_{M1} labeling. Dissociated blastomeres were reoriented such that their apical surfaces were in contact or the apical surface of one blastomeres was contacting the basolateral surface of another. Preliminary analysis was performed on G_{M1} localization at the new contact site. Results were inconsistent, showing G_{M1} clearing from the new contact site in some trials. Stacks through the Z plane were also taken in attempt to clarify results, but G_{M1} clearing was not easily analyzed.

Timing of G_{M1} mobility during ML-7 treatment in dissociated blastomeres has also been analyzed. Fifteen minutes after ML-7 treatment G_{M1} redistributes around the entire membrane, but after washout, it takes four times as long for G_{M1} localization to recover: 60 minutes. More interestingly, during this analysis, it was discovered that G_{M1} recovery after ML-7 washout was to its original apical localization. This result is

consistent and suggests a sort of “memory” retained in the membrane cortex during myosin light chain kinase inhibition. I now ask what are possible candidates for G_{M1} or membrane domain memory to the apical cell surface.

Since I have shown a significant role for myosin filaments in membrane cortex spatial control, I would examine myosin and associated proteins for their localization patterns during ML-7 treatment. Although myosin filament assembly is disrupted with ML-7 treatment, the distribution of myosin or myosin light chain kinase during this inhibition is not clear. The construct for a fluorescently labeled myosin light chain (received from T. Mizutani, Hokkaido University, Sapporo, Japan) could be used to examine myosin movement in live cells treated with ML-7. The correlation between myosin distribution and the cell cycle could be more closely examined.

In addition, Lifeact, a novel actin binding probe for use in live cells (Riedl et al., 2008), can be used to track actin mobility in sea urchin embryonic cells. Actin depolymerization by cytochalasin D or Latrunculin B did not affect G_{M1} localization or mobility. Lifeact could be used to examine actin mobility during the cell cycle and upon dissociation to confirm the stability of this meshwork in blastomeres.

Finally, analysis of membrane domains would be interesting in deciphering the interaction between myosin, G_{M1} , and the Par complex. Lipid rafts have been successfully isolated in sea urchin eggs and embryos (Ng et al., 2005; Belton et al., 2001) allowing for the characterization of membrane domains under various inhibitor treatments. In fact, Ishmael et al. (2007) found two nonmuscle myosin isoforms as components of detergent-resistant membrane domains, along with spectrins, actin, and tubulin subunits. Possible scaffolding proteins connecting the membrane to underlying

myosin could be identified by mass spectrophotometry. Binding partners of myosin II, such as supervillin, may be responsible for connecting the membrane to the cell cortex (Nebl et al., 2002; Chen et al., 2003).

Annexin XIIIb, associated with lipid microdomains, is involved in apical cellular trafficking and is an interesting candidate to examine in sea urchins for a role in polarizing membrane domains (Fiedler et al., 1995; Lafont et al., 1998; Nguyen et al., 2006). A recent search of the *S. purpuratus* genome for annexin XIIIb resulted in several hits worth investigating by immunofluorescence and western blot with established antibodies (Massey-Harroche et al., 1998)

In this thesis, I have initiated the characterization and analysis of precocious cell and embryonic polarity in cleavage stage sea urchin embryos and identified myosin filaments as the major regulator of membrane cortex polarity. Membrane domains and cortical polarity determinants are differentially regulated with respect to blastomere dissociation and investigation into the contact sites in early embryos will provide insight. Future studies in cell biology addressing the connection between the membrane cortex and nonmuscle myosin II will lead to a greater understanding of the maintenance of embryonic and cell polarity in cleavage stage sea urchin embryos.

Chapter 5: Materials and Methods

Sea Urchin Embryo Culture

Gametes from the sea urchins *Strongylocentrotus purpuratus* and *Lytechinus pictus* (Marinus, Long Beach, CA) were obtained by intracoelomic injection of 0.5 M KCl to induce shedding. The jelly coat of eggs was activated by allowing them to settle two times in artificial seawater (Instant Ocean, Aquarium Systems) after swirling. The eggs were fertilized by adding 1000X diluted sperm dropwise to eggs in sea water containing 4mM para-aminobenzoic acid (PABA). Fertilization was confirmed by the presence of fertilization envelopes. *S. purpuratus* eggs were pelleted in a low velocity manual centrifuge immediately following fertilization and resuspended in 1M urea. To remove fertilization envelopes, the eggs were passed through 73 μ m and 150 μ m nytex for *S. purpuratus* and *L. pictus*, respectively, two to three times. Fertilized eggs were cultured in either ASW or CaFSW at 10-15°C for *S. purpuratus* and 15-20°C for *L. pictus*.

Drug Treatments

Cytochalasin D (10 μ g/ml; Sigma, St. Louis, MO), blebbistatin (30 μ M; Calbiochem, La Jolla, CA), ML-7 (50-100 μ M; Sigma), Nocodazole (0.01-.1 μ M; Sigma), Latrunculin B (0.2 μ M; Calbiochem), ML-9 (120 μ M; Calbiochem), H1152 (2.5 μ g/ml; Alexis/Axxora, San Diego, CA) and myristolated protein kinase C zeta peptide inhibitor (4 μ M, reconstituted in dH₂O, BioMol, Plymouth Meeting, PA; Zhou et al, 1997; Ward and O'Brian 1993) were added to embryos at various cell stages as indicated in the text.

G_{M1} Labeling

For G_{M1} staining, Alexa 488 conjugated cholera toxin, subunit B (CTB) (5µg/ml, Molecular Probes) was added to live cells 30 minutes post-fertilization and washed out prior to imaging with 3 rinses of CaFSW. Alternatively, CTB was added to cells after the first division or after 2 or 4 cell stage embryos were dissociated by washing in CaFSW. For G_{M1} and *FAST* DiI experiments, cells were labeled with Alexa 488 CTB at 30 minutes post-fertilization as described above. At the 2 cell stage, the blastomeres were dissociated with gentle pipetting. For FRAP experiments, cell were labeled 15-20 minutes post-fertilization and CTB-488 was washed out 5 minutes prior to photobleaching.

Fixation and Immunostaining of PAR6, Cdc42 and aPKC

Prior to fixation, embryos were washed three times with a 19:1 mixture of 0.56M NaCl to KCl (Kane, 1986). Embryos were fixed in a 3.7% formaldehyde solution in water with 80mM PIPES, 1M glycerol, 5mM EGTA, and 5mM MgCl₂ for one hour rotating at room temperature. They were then permeabilized in the fix solution previously mentioned with the addition of 0.1% NP-40 for 20 minutes rotating at room temperature. Primary antibody, polyclonal goat-anti-PAR6 (1:100; Santa Cruz, sc-14405), polyclonal goat-anti-Cdc42 (1:50; Santa Cruz, sc-34314), or rabbit-anti-PKC-zeta (1:100; specific for both aPKC-zeta and aPKC-lambda, Santa Cruz, sc-216) was added to embryos in PBS, 0.1% Triton-X100 and were rotated overnight at 4°C. (For primary antibody specificity, see Supplemental figure 1.) Embryos were washed 3 times (20 minutes) with PBS, 0.1% Triton-X100. Secondary antibody, Alexa 488 labeled donkey anti-goat (for PAR6 and

Cdc42 primary antibodies) or mouse anti-rabbit (for PKC-zeta primary) (1:1000, Molecular Probes) in PBS, 0.1% Triton-X100, was added to the embryos and rotated overnight at 4°C.

Fixation and Immunostaining of Myosin II

Embryos were raised to the desired stage in CaFSW and fixed in Millonig's Phosphate Buffered Fixative (3% formaldehyde, 0.2M NaH₂PO₄*H₂O, 0.136M NaCl, pH 7.0) for 30 minutes rocking end-over-end at room temperature. Embryos were subsequently permeabilized in PBS, 0.5% Triton-X100 for 15 minutes at room temperature. Primary antibody, rabbit-anti-*S. purpuratus* egg myosin II (1:500, David Burgess) in PBS, 0.1% Triton-X100, was incubated with the embryos rotating for 1-2 hours at room temperature. Secondary antibody, Alexa 488 labeled anti-rabbit (1:1000, Molecular Probes) in PBS, 0.1% Triton-X100, was added to embryos, after 3 washes in PBS, 0.1% Triton-X100, for 1 hour rotating at room temperature.

Co-Immunoprecipitation

Pelleted embryos were lysed in RIPA buffer (150mM NaCl, 1% NP-40, 0.5% deoxycholic acid, 0.1% SDS, 50mM Tris) for 30 minutes on ice, with occasional mixing, in a volume of 1mL. The lysate was centrifuged for 10 minutes at 10,000xg at 4°C and the supernatant was collected. 4µg rabbit-anti-aPKC-zeta antibody (Santa Cruz, sc-216) was added to the lysate followed by 100µL µMACS Protein A microbeads. The mixture was incubated overnight at 4°C. The µ Column was placed in the magnetic field of the µMACS Separator and was washed with RIPA buffer. The lysate was applied to the

column, rinsed 4 times with RIPA buffer, and eluted with pre-heated (95°C) 1X SDS gel loading buffer (50mM Tris HCl (pH 6.8), 50mM DTT, 1% SDS, 0.005% bromophenol blue, 10% glycerol). The eluted precipitate was analyzed by SDS-PAGE and Western blot.

Fixation and Immunostaining of Microtubules

Embryos were allowed to settle and adhere to poly-L-lysine coated coverslips prior to fixation. Coverslips were then placed in ice cold methanol with the addition of 50mM EGTA for 5 minutes followed by 3 rinses with PBS. Coverslips with fixed embryos were blocked with immunofluorescence blocking buffer, IMF BB (2% goat serum and 1% bovine serum) for 1 hour at room temperature. Primary antibody DM1A monoclonal anti-alpha-tubulin (1:400, Sigma, St. Louis, MO; (Henson et al., 2008) in IMF BB was added directly to the coverslips for one hour at room temperature. Secondary antibody Alexa 488 labeled goat anti-mouse (1:400; Molecular Probes, Carlsbad, CA) in IMF BB was added directly to coverslips overnight at room temperature.

Endocytosis Assays

Alexa 488 CTB-stained embryos (as previously described) were dissociated in CaFSW at the 4 or 8 cell stage and concentrated to 1 ml in seawater. 90µl tetramethylrhodamine dextran (10mg/ml) was added to the dissociated blastomeres and incubated rotating 10 minutes at room temperature. Blastomeres were rinsed thoroughly with CaFSW 5 times prior to imaging of vesicles. Myristolated protein kinase C zeta peptide inhibitor (4µM, BioMol, Plymouth Meeting, PA) or cytochalasin D (10µM; Sigma, St. Louis, MO) were

added to the 1 ml culture of dissociated blastomeres for 10 minutes prior to the addition of tetramethylrhodamine dextran.

Isolation of Detergent Resistant Membranes (DRMs)

DRMs were obtained following protocols previously used in sea urchins (Belton et al., 2001; Ng et al., 2005).

Microscopy

For widefield microscopy, digital images were obtained on a Nikon TE 200 or TE 2000 inverted microscope equipped with a Hamamatsu Orca ER CCD camera driven by Metamorph software (Universal Imaging) using Nikon Plan Fluor 0.60 NA 40x and 0.45 NA 20x air objective lenses at room temperature. A Metamorph driven Uniblitz (Vincent Associates) shutter was used to control brightfield and either an Efos or Sutter smart shutter was used to control epifluorescence illumination. For spinning disk confocal microscopy, images were obtained on a Nikon TE 2000 inverted microscope with a Yokogawa spinning disk head and Prarie lasers (561 and 488) controlled by Metamorph software. A Brooke cooling stage was used to maintain a constant temperature for live cell timelapse experiments. For confocal microscopy, digital images were obtained on a Leica DM IRBE inverted scope equipped with the Leica TCSSP2 or TCSSP5 confocal system, using N PLAN 20x air, HCX PL APO 40x oil, and HCX PL APO 63x oil objective lenses. Leica confocal software was used to acquire and quantitate images.

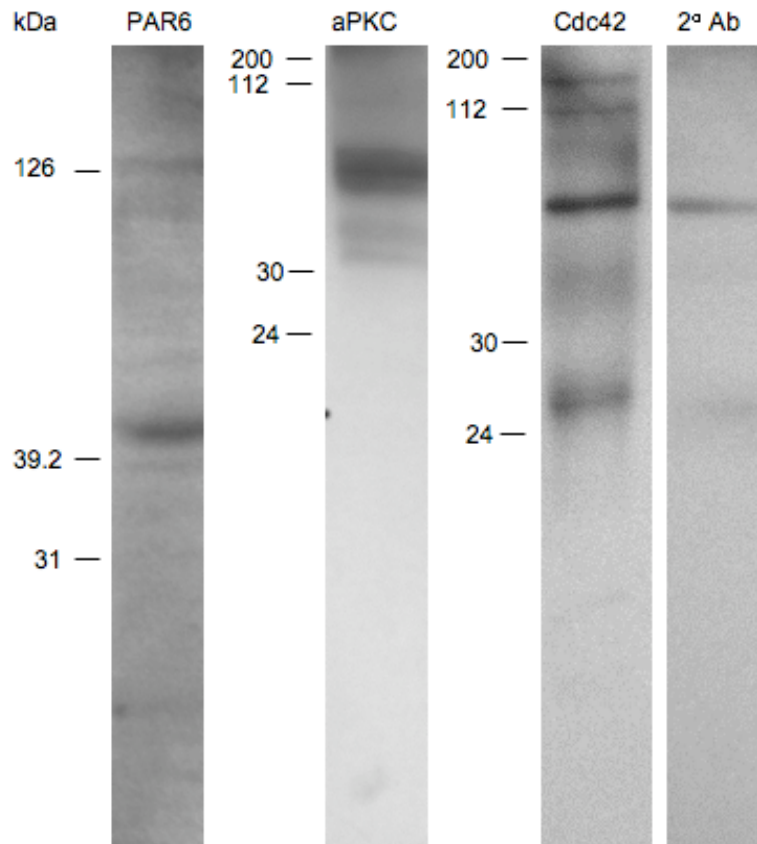
Fluorescence Recovery After Photobleaching (FRAP) Analysis

FRAP experiments were performed on a confocal microscope (described above) using the FRAP Wizard. Fluorescence intensities were analyzed using the Leica Application Suite software, Advanced Fluorescence and values were normalized to a region of interest (ROI) of equivalent size which was not bleached (*control*) and the background (*bkgd*) as follows:

$$100 \quad \times \quad \frac{F_{\text{ROI}} - F_{\text{bkgd}}}{F_{\text{control}} - F_{\text{bkgd}}} \quad \times \quad \frac{F_{\text{control (prebleach avg.)}} - F_{\text{bkgd}}}{F_{\text{ROI (prebleach avg.)}} - F_{\text{bkgd}}}$$

This normalization corrects for variation in staining for different treatments, background fluorescence, and loss of fluorescence during the bleach-recovery period. Recovery was designated as 40% of the loss of fluorescence photobleached at the ROI. A fluorescence intensity increase of 40% or greater compared to that which was lost, seen at anaphase, was set as the threshold for recovery.

Supplementary Figure 1



Supplemental Figure 1. Western blot analysis of primary antibodies demonstrate useable specificity for co-immunoprecipitation and immunofluorescence. Western blot of whole-cell extracts from 2 cell stage embryos shows specific detection of PAR6 at 43kDa, aPKC at 80kDa, and Cdc-42 at 25kDa. The secondary anti-rabbit-HRP antibody non-specifically binds to the embryo lysate, explaining the second arbitrary band in the Cdc42 lane (same blot).

Chapter 6: References

- Aceto, D., Beers, M., and Kemphues, K.J. (2006). Interaction of PAR-6 with CDC-42 is required for maintenance but not establishment of PAR asymmetry in *C. elegans*. *Dev. Biol.* *299*, 386-397.
- Albertson, R., Riggs, B., and Sullivan, W. (2005). Membrane traffic: a driving force in cytokinesis. *Trends Cell Biol.* *15*, 92-101.
- Alford, L.M., Ng, M.M., and Burgess, D.R. (2009). Cell polarity emerges at first cleavage in sea urchin embryos. *Dev. Biol.* *330*, 12-20.
- Anderson, D.C., Gill, J.S., Cinalli, R.M., and Nance, J. (2008). Polarization of the *C. elegans* embryo by RhoGAP-mediated exclusion of PAR-6 from cell contacts. *Science* *320*, 1771-1774.
- Andreuccetti, P., Barone Lumaga, M.R., Cafiero, G., Filosa, S., and Parisi, E. (1987). Cell junctions during the early development of the sea urchin embryo (*Paracentrotus lividus*). *Cell Differ.* *20*, 137-146.
- Atwood, S.X., Chabu, C., Penkert, R.R., Doe, C.Q., and Prehoda, K.E. (2007). Cdc42 acts downstream of Bazooka to regulate neuroblast polarity through Par-6 aPKC. *J. Cell. Sci.* *120*, 3200-3206.
- Atwood, S.X., and Prehoda, K.E. (2009). aPKC phosphorylates Miranda to polarize fate determinants during neuroblast asymmetric cell division. *Curr. Biol.* *19*, 723-729.
- Bagnat, M., and Simons, K. (2002). Cell surface polarization during yeast mating. *Proc. Natl. Acad. Sci. U. S. A.* *99*, 14183-14188.
- Barros, C.S., Phelps, C.B., and Brand, A.H. (2003). *Drosophila* nonmuscle myosin II promotes the asymmetric segregation of cell fate determinants by cortical exclusion rather than active transport. *Dev. Cell.* *5*, 829-840.
- Belton, R.J., Jr, Adams, N.L., and Foltz, K.R. (2001). Isolation and characterization of sea urchin egg lipid rafts and their possible function during fertilization. *Mol. Reprod. Dev.* *59*, 294-305.
- Bement, W.M., Benink, H.A., and von Dassow, G. (2005). A microtubule-dependent zone of active RhoA during cleavage plane specification. *J. Cell Biol.* *170*, 91-101.
- Bement, W.M., Yu, H.Y., Burkel, B.M., Vaughan, E.M., and Clark, A.G. (2007). Rehabilitation and the single cell. *Curr. Opin. Cell Biol.* *19*, 95-100.

- Betschinger, J., Mechtler, K., and Knoblich, J.A. (2003). The Par complex directs asymmetric cell division by phosphorylating the cytoskeletal protein Lgl. *Nature* *422*, 326-330.
- Bluemink, J.G., and de Laat, S.W. (1973). New membrane formation during cytokinesis in normal and cytochalasin B-treated eggs of *Xenopus laevis*. I. Electron microscope observations. *J. Cell Biol.* *59*, 89-108.
- Bowerman, B., and Severson, A.F. (1999). Cell division: plant-like properties of animal cell cytokinesis. *Curr. Biol.* *9*, R658-60.
- Bre, M.H., Pepperkok, R., Hill, A.M., Levilliers, N., Ansorge, W., Stelzer, E.H., and Karsenti, E. (1990). Regulation of microtubule dynamics and nucleation during polarization in MDCK II cells. *J. Cell Biol.* *111*, 3013-3021.
- Bunnell, S.C., Hong, D.I., Kardon, J.R., Yamazaki, T., McGlade, C.J., Barr, V.A., and Samelson, L.E. (2002). T cell receptor ligation induces the formation of dynamically regulated signaling assemblies. *J. Cell Biol.* *158*, 1263-1275.
- Burgess, R.W., Deitcher, D.L., and Schwarz, T.L. (1997). The synaptic protein syntaxin1 is required for cellularization of *Drosophila* embryos. *J. Cell Biol.* *138*, 861-875.
- Burke, R.D., Murray, G., Rise, M., and Wang, D. (2004). Integrins on eggs: the betaC subunit is essential for formation of the cortical actin cytoskeleton in sea urchin eggs. *Dev. Biol.* *265*, 53-60.
- Byers, T.J., and Armstrong, P.B. (1986). Membrane protein redistribution during *Xenopus* first cleavage. *J. Cell Biol.* *102*, 2176-2184.
- Cardellini, P., Davanzo, G., and Citi, S. (1996). Tight junctions in early amphibian development: detection of junctional cingulin from the 2-cell stage and its localization at the boundary of distinct membrane domains in dividing blastomeres in low calcium. *Dev. Dyn.* *207*, 104-113.
- Chalmers, A.D., Strauss, B., and Papalopulu, N. (2003). Oriented cell divisions asymmetrically segregate aPKC and generate cell fate diversity in the early *Xenopus* embryo. *Development* *130*, 2657-2668.
- Chang, F., Feierbach, B., and Martin, S. (2005). Regulation of actin assembly by microtubules in fission yeast cell polarity. *Novartis found. Symp.* *269*, 59-66; discussion 66-72, 223-30.
- Chen, T.W., Chen, G., Funkhouser, L.J., and Nam, S.C. (2009). Membrane domain modulation by Spectrins in *Drosophila* photoreceptor morphogenesis. *Genesis*

- Chen, Y., Merzdorf, C., Paul, D.L., and Goodenough, D.A. (1997). COOH terminus of occludin is required for tight junction barrier function in early *Xenopus* embryos. *J. Cell Biol.* *138*, 891-899.
- Chen, Y., Takizawa, N., Crowley, J.L., Oh, S.W., Gatto, C.L., Kambara, T., Sato, O., Li, X.D., Ikebe, M., and Luna, E.J. (2003). F-actin and myosin II binding domains in supervillin. *J. Biol. Chem.* *278*, 46094-46106.
- Choi, S.C., Kim, J., and Han, J.K. (2000). Identification and developmental expression of par-6 gene in *Xenopus laevis*. *Mech. Dev.* *91*, 347-350.
- Clark, E.A., and Brugge, J.S. (1995). Integrins and signal transduction pathways: the road taken. *Science* *268*, 233-239.
- Conner, S.D., and Wessel, G.M. (1999). Syntaxin is required for cell division. *Mol. Biol. Cell* *10*, 2735-2743.
- Conti, M.A., and Adelstein, R.S. (2008). Nonmuscle myosin II moves in new directions. *J. Cell. Sci.* *121*, 11-18.
- Cowan, C.R., and Hyman, A.A. (2007). Acto-myosin reorganization and PAR polarity in *C. elegans*. *Development* *134*, 1035-1043.
- Cowan, C.R., and Hyman, A.A. (2004). Asymmetric cell division in *C. elegans*: cortical polarity and spindle positioning. *Annu. Rev. Cell Dev. Biol.* *20*, 427-453.
- Croce, J.C., and McClay, D.R. (2006). The canonical Wnt pathway in embryonic axis polarity. *Semin. Cell Dev. Biol.* *17*, 168-174.
- Dan, K. (1954) The cortical movement in *Arbacia* eggs through cleavage cycles. *Embryologia* *2*, 115-122.
- Dan, K. (1954) Further study on the formation of the "new membrane" in eggs of the sea urchin, *Hemicentrotus (Strongylocentrotus) pulcherrimus*. *Embryologia* *2*, 99-114.
- DAN, K. (1960). Cyto-embryology of echinoderms and amphibia. *Int. Rev. Cytol.* *9*, 321-367.
- Danilchik, M.V., Bedrick, S.D., Brown, E.E., and Ray, K. (2003). Furrow microtubules and localized exocytosis in cleaving *Xenopus laevis* embryos. *J. Cell. Sci.* *116*, 273-283.
- Danilchik, M.V., Funk, W.C., Brown, E.E., and Larkin, K. (1998). Requirement for microtubules in new membrane formation during cytokinesis of *Xenopus* embryos. *Dev. Biol.* *194*, 47-60.

- de Anda, F.C., Pollarolo, G., Da Silva, J.S., Camoletto, P.G., Feiguin, F., and Dotti, C.G. (2005). Centrosome localization determines neuronal polarity. *Nature* *436*, 704-708.
- De Lorenzo, C., Mechler, B.M., and Bryant, P.J. (1999). What is *Drosophila* telling us about cancer? *Cancer Metastasis Rev.* *18*, 295-311.
- Doe, C.Q. (2001). Cell polarity: the PARty expands. *Nat. Cell Biol.* *3*, E7-9.
- Doe, C.Q., and Bowerman, B. (2001). Asymmetric cell division: fly neuroblast meets worm zygote. *Curr. Opin. Cell Biol.* *13*, 68-75.
- Drubin, D.G., and Nelson, W.J. (1996). Origins of cell polarity. *Cell* *84*, 335-344.
- D'Souza-Schorey, C., and Chavrier, P. (2006). ARF proteins: roles in membrane traffic and beyond. *Nat. Rev. Mol. Cell Biol.* *7*, 347-358.
- Duncan, F.E., Moss, S.B., Schultz, R.M., and Williams, C.J. (2005). PAR-3 defines a central subdomain of the cortical actin cap in mouse eggs. *Dev. Biol.* *280*, 38-47.
- Eddy, R.J., Pierini, L.M., Matsumura, F., and Maxfield, F.R. (2000). Ca²⁺-dependent myosin II activation is required for uropod retraction during neutrophil migration. *J. Cell. Sci.* *113 (Pt 7)*, 1287-1298.
- Etemad-Moghadam, B., Guo, S., and Kemphues, K.J. (1995). Asymmetrically distributed PAR-3 protein contributes to cell polarity and spindle alignment in early *C. elegans* embryos. *Cell* *83*, 743-752.
- Feng, B., Schwarz, H., and Jesuthasan, S. (2002). Furrow-specific endocytosis during cytokinesis of zebrafish blastomeres. *Exp. Cell Res.* *279*, 14-20.
- Fesenko, I., Kurth, T., Sheth, B., Fleming, T.P., Citi, S., and Hausen, P. (2000). Tight junction biogenesis in the early *Xenopus* embryo. *Mech. Dev.* *96*, 51-65.
- Fiedler, K., Lafont, F., Parton, R.G., and Simons, K. (1995). Annexin XIIIb: a novel epithelial specific annexin is implicated in vesicular traffic to the apical plasma membrane. *J. Cell Biol.* *128*, 1043-1053.
- Finger, F.P., and White, J.G. (2002). Fusion and fission: membrane trafficking in animal cytokinesis. *Cell* *108*, 727-730.
- Fischer, R., Zekert, N., and Takeshita, N. (2008). Polarized growth in fungi--interplay between the cytoskeleton, positional markers and membrane domains. *Mol. Microbiol.* *68*, 813-826.

- Fleming, T.P., Papenbrock, T., Fesenko, I., Hausen, P., and Sheth, B. (2000). Assembly of tight junctions during early vertebrate development. *Semin. Cell Dev. Biol.* *11*, 291-299.
- Gao, L., and Macara, I.G. (2004). Isoforms of the polarity protein par6 have distinct functions. *J. Biol. Chem.* *279*, 41557-41562.
- Garrard, S.M., Capaldo, C.T., Gao, L., Rosen, M.K., Macara, I.G., and Tomchick, D.R. (2003). Structure of Cdc42 in a complex with the GTPase-binding domain of the cell polarity protein, Par6. *EMBO J.* *22*, 1125-1133.
- Gawantka, V., Ellinger-Ziegelbauer, H., and Hausen, P. (1992). Beta 1-integrin is a maternal protein that is inserted into all newly formed plasma membranes during early *Xenopus* embryogenesis. *Development* *115*, 595-605.
- Gomez-Mouton, C., Abad, J.L., Mira, E., Lacalle, R.A., Gallardo, E., Jimenez-Baranda, S., Illa, I., Bernad, A., Manes, S., and Martinez-A, C. (2001). Segregation of leading-edge and uropod components into specific lipid rafts during T cell polarization. *Proc. Natl. Acad. Sci. U. S. A.* *98*, 9642-9647.
- Gotta, M., Abraham, M.C., and Ahringer, J. (2001). CDC-42 controls early cell polarity and spindle orientation in *C. elegans*. *Curr. Biol.* *11*, 482-488.
- Gundersen, G.G., Kreitzer, G., Cook, T., and Liao, G. (1998). Microtubules as determinants of cellular polarity. *Biol. Bull.* *194*, 358-360.
- Guo, S., and Kemphues, K.J. (1996). A non-muscle myosin required for embryonic polarity in *Caenorhabditis elegans*. *Nature* *382*, 455-458.
- Guo, S., and Kemphues, K.J. (1995). par-1, a gene required for establishing polarity in *C. elegans* embryos, encodes a putative Ser/Thr kinase that is asymmetrically distributed. *Cell* *81*, 611-620.
- Gurland, G., and Gundersen, G.G. (1995). Stable, detyrosinated microtubules function to localize vimentin intermediate filaments in fibroblasts. *J. Cell Biol.* *131*, 1275-1290.
- Harder, T., and Kuhn, M. (2000). Selective accumulation of raft-associated membrane protein LAT in T cell receptor signaling assemblies. *J. Cell Biol.* *151*, 199-208.
- Harder, T., and Simons, K. (1999). Clusters of glycolipid and glycosylphosphatidylinositol-anchored proteins in lymphoid cells: accumulation of actin regulated by local tyrosine phosphorylation. *Eur. J. Immunol.* *29*, 556-562.
- Henrique, D., and Schweisguth, F. (2003). Cell polarity: the ups and downs of the Par6/aPKC complex. *Curr. Opin. Genet. Dev.* *13*, 341-350.

Henson, J.H., Fried, C.A., McClellan, M.K., Ader, J., Davis, J.E., Oldenbourg, R., and Simerly, C.R. (2008). Bipolar, anastral spindle development in artificially activated sea urchin eggs. *Dev. Dyn.* 237, 1348-1358.

Hickson, G.R., Matheson, J., Riggs, B., Maier, V.H., Fielding, A.B., Prekeris, R., Sullivan, W., Barr, F.A., and Gould, G.W. (2003). Arfophilins are dual Arf/Rab 11 binding proteins that regulate recycling endosome distribution and are related to *Drosophila* nuclear fallout. *Mol. Biol. Cell* 14, 2908-2920.

Hill, D.P., and Strome, S. (1990). Brief cytochalasin-induced disruption of microfilaments during a critical interval in 1-cell *C. elegans* embryos alters the partitioning of developmental instructions to the 2-cell embryo. *Development* 108, 159-172.

Hill, D.P., and Strome, S. (1988). An analysis of the role of microfilaments in the establishment and maintenance of asymmetry in *Caenorhabditis elegans* zygotes. *Dev. Biol.* 125, 75-84.

Hörstadius, S. (1973). *Experimental embryology of echinoderms* (Oxford Eng.: Clarendon Press).

Hu, Q., Nelson, W.J., and Spiliotis, E.T. (2008). Forchlorfenuron alters mammalian septin assembly, organization, and dynamics. *J. Biol. Chem.* 283, 29563-29571.

Hutterer, A., Betschinger, J., Petronczki, M., and Knoblich, J.A. (2004). Sequential roles of Cdc42, Par-6, aPKC, and Lgl in the establishment of epithelial polarity during *Drosophila* embryogenesis. *Dev. Cell.* 6, 845-854.

Hyodo-Miura, J., Yamamoto, T.S., Hyodo, A.C., Iemura, S., Kusakabe, M., Nishida, E., Natsume, T., and Ueno, N. (2006). XGAP, an ArfGAP, is required for polarized localization of PAR proteins and cell polarity in *Xenopus* gastrulation. *Dev. Cell.* 11, 69-79.

Inoue, S. (1990) Dynamics of Mitosis and Cleavage. *Ann. N.Y. Acad. Sci.* 582, 1-14.

Ishmael, J.E., Safic, M., Amparan, D., Vogel, W.K., Pham, T., Marley, K., Filtz, T.M., and Maier, C.S. (2007). Nonmuscle myosins II-B and Va are components of detergent-resistant membrane skeletons derived from mouse forebrain. *Brain Res.* 1143, 46-59.

Jantsch-Plunger, V., and Glotzer, M. (1999). Depletion of syntaxins in the early *Caenorhabditis elegans* embryo reveals a role for membrane fusion events in cytokinesis. *Curr. Biol.* 9, 738-745.

Jenkins, N., Saam, J.R., and Mango, S.E. (2006). CYK-4/GAP provides a localized cue to initiate anteroposterior polarity upon fertilization. *Science* 313, 1298-1301.

- Kalmes, A., Merdes, G., Neumann, B., Strand, D., and Mechler, B.M. (1996). A serine-kinase associated with the p127-l(2)gl tumour suppressor of *Drosophila* may regulate the binding of p127 to nonmuscle myosin II heavy chain and the attachment of p127 to the plasma membrane. *J. Cell. Sci.* *109 (Pt 6)*, 1359-1368.
- Kane, R.E. (1973). Hyalin release during normal sea urchin development and its replacement after removal at fertilization. *Exp. Cell Res.* *81*, 301-311.
- Kay, A.J., and Hunter, C.P. (2001). CDC-42 regulates PAR protein localization and function to control cellular and embryonic polarity in *C. elegans*. *Curr. Biol.* *11*, 474-481.
- Kolega, J. (2003). Asymmetric distribution of myosin IIB in migrating endothelial cells is regulated by a rho-dependent kinase and contributes to tail retraction. *Mol. Biol. Cell* *14*, 4745-4757.
- Kuraishi, R., and Osanai, K. (1989). Structural and functional polarity of starfish blastomeres. *Dev. Biol.* *136*, 304-310.
- Lafont, F., Lecat, S., Verkade, P., and Simons, K. (1998). Annexin XIIIb associates with lipid microdomains to function in apical delivery. *J. Cell Biol.* *142*, 1413-1427.
- Lecuit, T., and Wieschaus, E. (2000). Polarized insertion of new membrane from a cytoplasmic reservoir during cleavage of the *Drosophila* embryo. *J. Cell Biol.* *150*, 849-860.
- Li, R., and Gundersen, G.G. (2008). Beyond polymer polarity: how the cytoskeleton builds a polarized cell. *Nat. Rev. Mol. Cell Biol.* *9*, 860-873.
- Liao, G., and Gundersen, G.G. (1998). Kinesin is a candidate for cross-bridging microtubules and intermediate filaments. Selective binding of kinesin to deetyrosinated tubulin and vimentin. *J. Biol. Chem.* *273*, 9797-9803.
- Lucero, A., Stack, C., Bresnick, A.R., and Shuster, C.B. (2006). A global, myosin light chain kinase-dependent increase in myosin II contractility accompanies the metaphase-anaphase transition in sea urchin eggs. *Mol. Biol. Cell* *17*, 4093-4104.
- Manes, S., Mira, E., Gomez-Mouton, C., Lacalle, R.A., Keller, P., Labrador, J.P., and Martinez-A, C. (1999). Membrane raft microdomains mediate front-rear polarity in migrating cells. *EMBO J.* *18*, 6211-6220.
- Martin-Belmonte, F., and Mostov, K. (2008). Regulation of cell polarity during epithelial morphogenesis. *Curr. Opin. Cell Biol.* *20*, 227-234.
- Massey-Harroche, D., Mayran, N., and Maroux, S. (1998). Polarized localizations of annexins I, II, VI and XIII in epithelial cells of intestinal, hepatic and pancreatic tissues. *J. Cell. Sci.* *111 (Pt 20)*, 3007-3015.

- Mata, J., and Nurse, P. (1997). Tea1 and the Microtubular Cytoskeleton are Important for Generating Global Spatial Order within the Fission Yeast Cell. *Cell* 89, 939-949.
- Mata, J., and Nurse, P. (1997). Tea1 and the Microtubular Cytoskeleton are Important for Generating Global Spatial Order within the Fission Yeast Cell. *Cell* 89, 939-949.
- Matter, K. (2000). Epithelial polarity: sorting out the sorters. *Curr. Biol.* 10, R39-42.
- Mavrakis, M., Rikhy, R., and Lippincott-Schwartz, J. (2009). Plasma membrane polarity and compartmentalization are established before cellularization in the fly embryo. *Dev. Cell.* 16, 93-104.
- McCaig, C.D., and Robinson, K.R. (1982). The distribution of lectin receptors on the plasma membrane of the fertilized sea urchin egg during first and second cleavage. *Dev. Biol.* 92, 197-202.
- McMurray, M.A., and Thorner, J. (2009). Septins: molecular partitioning and the generation of cellular asymmetry. *Cell. Div.* 4, 18.
- Merzdorf, C.S., Chen, Y.H., and Goodenough, D.A. (1998). Formation of functional tight junctions in *Xenopus* embryos. *Dev. Biol.* 195, 187-203.
- Miller, J.R., and McClay, D.R. (1997). Changes in the pattern of adherens junction-associated beta-catenin accompany morphogenesis in the sea urchin embryo. *Dev. Biol.* 192, 310-322.
- Miller, J.R., and McClay, D.R. (1997). Characterization of the role of cadherin in regulating cell adhesion during sea urchin development. *Dev. Biol.* 192, 323-339.
- Muller, H.A., and Hausen, P. (1995). Epithelial cell polarity in early *Xenopus* development. *Dev. Dyn.* 202, 405-420.
- Munro, E.M. (2006). PAR proteins and the cytoskeleton: a marriage of equals. *Curr. Opin. Cell Biol.* 18, 86-94.
- Murthy, K., and Wadsworth, P. (2005). Myosin-II-dependent localization and dynamics of F-actin during cytokinesis. *Curr. Biol.* 15, 724-731.
- Nakaya, M., Fukui, A., Izumi, Y., Akimoto, K., Asashima, M., and Ohno, S. (2000). Meiotic maturation induces animal-vegetal asymmetric distribution of aPKC and ASIP/PAR-3 in *Xenopus* oocytes. *Development* 127, 5021-5031.
- Nakayama, Y., Shivas, J.M., Poole, D.S., Squirrell, J.M., Kulkoski, J.M., Schleede, J.B., and Skop, A.R. (2009). Dynamin participates in the maintenance of anterior polarity in the *Caenorhabditis elegans* embryo. *Dev. Cell.* 16, 889-900.

- Nebi, T., Pestonjamas, K.N., Leszyk, J.D., Crowley, J.L., Oh, S.W., and Luna, E.J. (2002). Proteomic analysis of a detergent-resistant membrane skeleton from neutrophil plasma membranes. *J. Biol. Chem.* *277*, 43399-43409.
- Nelson, S.H., and McClay, D.R. (1988). Cell polarity in sea urchin embryos: reorientation of cells occurs quickly in aggregates. *Dev. Biol.* *127*, 235-247.
- Ng, M.M., Chang, F., and Burgess, D.R. (2005). Movement of membrane domains and requirement of membrane signaling molecules for cytokinesis. *Dev. Cell.* *9*, 781-790.
- Nguyen, H.T., Amine, A.B., Lafitte, D., Waheed, A.A., Nicoletti, C., Villard, C., Letisse, M., Deyris, V., Roziere, M., Tchiakpe, L. *et al.* (2006). Proteomic characterization of lipid rafts markers from the rat intestinal brush border. *Biochem. Biophys. Res. Commun.* *342*, 236-244.
- Ohno, S. (2001). Intercellular junctions and cellular polarity: the PAR-aPKC complex, a conserved core cassette playing fundamental roles in cell polarity. *Curr. Opin. Cell Biol.* *13*, 641-648.
- Ohshiro, T., Yagami, T., Zhang, C., and Matsuzaki, F. (2000). Role of cortical tumour-suppressor proteins in asymmetric division of *Drosophila* neuroblast. *Nature* *408*, 593-596.
- Okazaki, K. (1975) Normal Development to Metamorphosis. In: G. Chizhak, Editor, *In the Sea Urchin Embryo*, 177-232.
- Oliferenko, S., Paiha, K., Harder, T., Gerke, V., Schwarzler, C., Schwarz, H., Beug, H., Gunthert, U., and Huber, L.A. (1999). Analysis of CD44-containing lipid rafts: Recruitment of annexin II and stabilization by the actin cytoskeleton. *J. Cell Biol.* *146*, 843-854.
- Ossipova, O., Ezan, J., and Sokol, S.Y. (2009). PAR-1 phosphorylates mind bomb to promote vertebrate neurogenesis. *Dev. Cell.* *17*, 222-233.
- Ossipova, O., Tabler, J., Green, J.B., and Sokol, S.Y. (2007). PAR1 specifies ciliated cells in vertebrate ectoderm downstream of aPKC. *Development* *134*, 4297-4306.
- Palazzo, A.F., Eng, C.H., Schlaepfer, D.D., Marcantonio, E.E., and Gundersen, G.G. (2004). Localized stabilization of microtubules by integrin- and FAK-facilitated Rho signaling. *Science* *303*, 836-839.
- Patalano, S., Pruliere, G., Prodon, F., Paix, A., Dru, P., Sardet, C., and Chenevert, J. (2006). The aPKC-PAR-6-PAR-3 cell polarity complex localizes to the centrosome attracting body, a macroscopic cortical structure responsible for asymmetric divisions in the early ascidian embryo. *J. Cell. Sci.* *119*, 1592-1603.

- Peng, C.Y., Manning, L., Albertson, R., and Doe, C.Q. (2000). The tumour-suppressor genes *lgl* and *dlg* regulate basal protein targeting in *Drosophila* neuroblasts. *Nature* *408*, 596-600.
- Phillips, H.M., Murdoch, J.N., Chaudhry, B., Copp, A.J., and Henderson, D.J. (2005). *Vangl2* acts via RhoA signaling to regulate polarized cell movements during development of the proximal outflow tract. *Circ. Res.* *96*, 292-299.
- Piekny, A., Werner, M., and Glotzer, M. (2005). Cytokinesis: welcome to the Rho zone. *Trends Cell Biol.* *15*, 651-658.
- Plusa, B., Frankenberg, S., Chalmers, A., Hadjantonakis, A.K., Moore, C.A., Papalopulu, N., Papaioannou, V.E., Glover, D.M., and Zernicka-Goetz, M. (2005). Downregulation of *Par3* and *aPKC* function directs cells towards the ICM in the preimplantation mouse embryo. *J. Cell. Sci.* *118*, 505-515.
- Qiu, R.G., Abo, A., and Steven Martin, G. (2000). A human homolog of the *C. elegans* polarity determinant *Par-6* links *Rac* and *Cdc42* to *PKCzeta* signaling and cell transformation. *Curr. Biol.* *10*, 697-707.
- Renner, M., Choquet, D., and Triller, A. (2009). Control of the postsynaptic membrane viscosity. *J. Neurosci.* *29*, 2926-2937.
- Riggs, B., Rothwell, W., Mische, S., Hickson, G.R., Matheson, J., Hays, T.S., Gould, G.W., and Sullivan, W. (2003). Actin cytoskeleton remodeling during early *Drosophila* furrow formation requires recycling endosomal components Nuclear-fallout and *Rab11*. *J. Cell Biol.* *163*, 143-154.
- Roberts, R.K., and Appel, B. (2009). Apical polarity protein *PrkCi* is necessary for maintenance of spinal cord precursors in zebrafish. *Dev. Dyn.* *238*, 1638-1648.
- Sampson, K., and Heath, I.B. (2005). The dynamic behaviour of microtubules and their contributions to hyphal tip growth in *Aspergillus nidulans*. *Microbiology* *151*, 1543-1555.
- Sapir, T., Shmueli, A., Levy, T., Timm, T., Elbaum, M., Mandelkow, E.M., and Reiner, O. (2008). Antagonistic effects of doublecortin and *MARK2/Par-1* in the developing cerebral cortex. *J. Neurosci.* *28*, 13008-13013.
- Schonegg, S., Constantinescu, A.T., Hoege, C., and Hyman, A.A. (2007). The Rho GTPase-activating proteins *RGA-3* and *RGA-4* are required to set the initial size of *PAR* domains in *Caenorhabditis elegans* one-cell embryos. *Proc. Natl. Acad. Sci. U. S. A.* *104*, 14976-14981.

Schonegg, S., and Hyman, A.A. (2006). CDC-42 and RHO-1 coordinate acto-myosin contractility and PAR protein localization during polarity establishment in *C. elegans* embryos. *Development* *133*, 3507-3516.

Schonegg, S., and Hyman, A.A. (2006). CDC-42 and RHO-1 coordinate acto-myosin contractility and PAR protein localization during polarity establishment in *C. elegans* embryos. *Development* *133*, 3507-3516.

Schroeder, T.E. (1988). Contact-independent polarization of the cell surface and cortex of free sea urchin blastomeres. *Dev. Biol.* *125*, 255-264.

Schuck, S., and Simons, K. (2004). Polarized sorting in epithelial cells: raft clustering and the biogenesis of the apical membrane. *J. Cell. Sci.* *117*, 5955-5964.

Severson, A.F., and Bowerman, B. (2003). Myosin and the PAR proteins polarize microfilament-dependent forces that shape and position mitotic spindles in *Caenorhabditis elegans*. *J. Cell Biol.* *161*, 21-26.

Shelton, C.A., Carter, J.C., Ellis, G.C., and Bowerman, B. (1999). The nonmuscle myosin regulatory light chain gene *mlc-4* is required for cytokinesis, anterior-posterior polarity, and body morphology during *Caenorhabditis elegans* embryogenesis. *J. Cell Biol.* *146*, 439-451.

Sheng, M., and Hoogenraad, C.C. (2007). The postsynaptic architecture of excitatory synapses: a more quantitative view. *Annu. Rev. Biochem.* *76*, 823-847.

Sherwood, D.R., and McClay, D.R. (1997). Identification and localization of a sea urchin Notch homologue: insights into vegetal plate regionalization and Notch receptor regulation. *Development* *124*, 3363-3374.

Shiomi, K., and Yamaguchi, M. (2008). Expression patterns of three Par-related genes in sea urchin embryos. *Gene Expr. Patterns* *8*, 323-330.

Shuster, C.B., and Burgess, D.R. (2002). Targeted new membrane addition in the cleavage furrow is a late, separate event in cytokinesis. *Proc. Natl. Acad. Sci. U. S. A.* *99*, 3633-3638.

Sisson, J.C., Field, C., Ventura, R., Royou, A., and Sullivan, W. (2000). Lava lamp, a novel peripheral golgi protein, is required for *Drosophila melanogaster* cellularization. *J. Cell Biol.* *151*, 905-918.

Skop, A.R., Bergmann, D., Mohler, W.A., and White, J.G. (2001). Completion of cytokinesis in *C. elegans* requires a brefeldin A-sensitive membrane accumulation at the cleavage furrow apex. *Curr. Biol.* *11*, 735-746.

- Skop, A.R., Liu, H., Yates, J., 3rd, Meyer, B.J., and Heald, R. (2004). Dissection of the mammalian midbody proteome reveals conserved cytokinesis mechanisms. *Science* *305*, 61-66.
- Spiegel, E., and Howard, L. (1983). Development of cell junctions in sea-urchin embryos. *J. Cell. Sci.* *62*, 27-48.
- Strickland, L.I., Donnelly, E.J., and Burgess, D.R. (2005). Induction of cytokinesis is independent of precisely regulated microtubule dynamics. *Mol. Biol. Cell* *16*, 4485-4494.
- Suzuki, A., and Ohno, S. (2006). The PAR-aPKC system: lessons in polarity. *J. Cell. Sci.* *119*, 979-987.
- Takahashi, S., and Pryciak, P.M. (2007). Identification of novel membrane-binding domains in multiple yeast Cdc42 effectors. *Mol. Biol. Cell* *18*, 4945-4956.
- Takeshita, N., Higashitsuji, Y., Konzack, S., and Fischer, R. (2008). Apical sterol-rich membranes are essential for localizing cell end markers that determine growth directionality in the filamentous fungus *Aspergillus nidulans*. *Mol. Biol. Cell* *19*, 339-351.
- Tanentzapf, G., and Tepass, U. (2003). Interactions between the crumbs, lethal giant larvae and bazooka pathways in epithelial polarization. *Nat. Cell Biol.* *5*, 46-52.
- Thomas, G.H. (2001). Spectrin: the ghost in the machine. *Bioessays* *23*, 152-160.
- Totsukawa, G., Wu, Y., Sasaki, Y., Hartshorne, D.J., Yamakita, Y., Yamashiro, S., and Matsumura, F. (2004). Distinct roles of MLCK and ROCK in the regulation of membrane protrusions and focal adhesion dynamics during cell migration of fibroblasts. *J. Cell Biol.* *164*, 427-439.
- Triller, A., and Choquet, D. (2008). New concepts in synaptic biology derived from single-molecule imaging. *Neuron* *59*, 359-374.
- Triller, A., and Choquet, D. (2005). Surface trafficking of receptors between synaptic and extrasynaptic membranes: and yet they do move! *Trends Neurosci.* *28*, 133-139.
- Vinot, S., Le, T., Ohno, S., Pawson, T., Maro, B., and Louvet-Vallee, S. (2005). Asymmetric distribution of PAR proteins in the mouse embryo begins at the 8-cell stage during compaction. *Dev. Biol.* *282*, 307-319.
- von Trotha, J.W., Campos-Ortega, J.A., and Reugels, A.M. (2006). Apical localization of ASIP/PAR-3:EGFP in zebrafish neuroepithelial cells involves the oligomerization domain CR1, the PDZ domains, and the C-terminal portion of the protein. *Dev. Dyn.* *235*, 967-977.

- Walker, G.R., Kane, R., and Burgess, D.R. (1994). Isolation and characterization of a sea urchin zygote cortex that supports in vitro contraction and reactivation of furrowing. *J. Cell. Sci.* *107* (Pt 8), 2239-2248.
- Ward, N.E., and O'Brian, C.A. (1993). Inhibition of protein kinase C by N-myristoylated peptide substrate analogs. *Biochemistry* *32*, 11903-11909.
- Weirich, C.S., Erzberger, J.P., and Barral, Y. (2008). The septin family of GTPases: architecture and dynamics. *Nat. Rev. Mol. Cell Biol.* *9*, 478-489.
- Wenger, J., Gerard, D., Lenne, P.F., Rigneault, H., Dintinger, J., Ebbesen, T.W., Boned, A., Conchonaud, F., and Marguet, D. (2006). Dual-color fluorescence cross-correlation spectroscopy in a single nanoaperture : towards rapid multicomponent screening at high concentrations. *Opt. Express* *14*, 12206-12216.
- Whalley, T., Terasaki, M., Cho, M.S., and Vogel, S.S. (1995). Direct membrane retrieval into large vesicles after exocytosis in sea urchin eggs. *J. Cell Biol.* *131*, 1183-1192.
- Wirtz-Peitz, F., Nishimura, T., and Knoblich, J.A. (2008). Linking cell cycle to asymmetric division: Aurora-A phosphorylates the Par complex to regulate Numb localization. *Cell* *135*, 161-173.
- Wulfing, C., Bauch, A., Crabtree, G.R., and Davis, M.M. (2000). The vav exchange factor is an essential regulator in actin-dependent receptor translocation to the lymphocyte-antigen-presenting cell interface. *Proc. Natl. Acad. Sci. U. S. A.* *97*, 10150-10155.
- Yeaman, C., Grindstaff, K.K., Hansen, M.D., and Nelson, W.J. (1999). Cell polarity: Versatile scaffolds keep things in place. *Curr. Biol.* *9*, R515-7.
- Zernicka-Goetz, M. (2005). Cleavage pattern and emerging asymmetry of the mouse embryo. *Nat. Rev. Mol. Cell Biol.* *6*, 919-928.
- Zhou, G., Seibenhener, M.L., and Wooten, M.W. (1997). Nucleolin is a protein kinase C-zeta substrate. Connection between cell surface signaling and nucleus in PC12 cells. *J. Biol. Chem.* *272*, 31130-31137.